1 Connectomic Analysis of the *Drosophila* Lateral Neuron Clock Cells

2 **Reveals the Synaptic Basis of Functional Pacemaker Classes**

3

Shafer, O.T.^{1,*}, Gutierrez G.J.^{2,*}, Li, K.³, Mildenhall, A.³, Spira, D.^{2,3}, Marty, J.⁴, Lazar, A.A.⁴, and
 Fernandez M.P.^{3,#}

6 7

8 1- Advanced Science Research Center, Graduate Center, The City University of New York. New York, NY 10031

9 2- Center for Theoretical Neuroscience, Zuckerman Institute, Columbia University. New York, NY 10027

10 3- Department of Neuroscience and Behavior, Barnard College. New York, NY 10027

11 4- Department of Electrical Engineering, Columbia University. New York, NY 10027

12 13 *Equal contribution

[#]Correspondence should be submitted to Maria Paz Fernandez (mfernand@barnard.edu)

15

16

17 Abstract

18 The circadian clock orchestrates daily changes in physiology and behavior to ensure internal 19 temporal order and optimal timing across the day. In animals, a central brain clock coordinates 20 circadian rhythms throughout the body and is characterized by a remarkable robustness that 21 depends on synaptic connections between constituent neurons. The clock neuron network of 22 Drosophila, which shares network motifs with clock networks in the mammalian brain yet is built 23 of many fewer neurons, offers a powerful model for understanding the network properties of 24 circadian timekeeping. Here we report an assessment of synaptic connectivity within a clock 25 network, focusing on the critical lateral neuron (LN) clock neuron classes. Our results reveal that 26 previously identified anatomical and functional subclasses of LNs represent distinct 27 connectomic types. Moreover, we identify a small number of clock cell subtypes representing 28 highly synaptically coupled nodes within the clock neuron network. This suggests that neurons 29 lacking molecular timekeeping likely play integral roles within the circadian timekeeping network. 30 To our knowledge, this represents the first comprehensive connectomic analysis of a circadian 31 neuronal network.

32 Introduction

33

34 Most organisms undergo predictable daily changes in gene expression, physiology, and 35 behavior that are driven by endogenous circadian clocks (1, 2). In animals, the molecular 36 feedback loops underlying circadian clocks are present in all organ systems but are required 37 within a relatively small population of brain neurons to maintain daily rhythms in behavior and 38 physiology (3). In mammals, the hypothalamic suprachiasmatic nuclei (SCN) are the brain's 39 central circadian clock since the ablation of the SCN or knockouts of the molecular clock within 40 the SCN results in loss of circadian rhythms (reviewed by (4)). Compared to peripheral tissues, 41 timekeeping in the brain's central clock is more resilient to the loss of clock gene function and to 42 environmental perturbations. This resilience comes from physiological connections between 43 SCN neurons (5, 6). Determining how clock neurons are connected is therefore essential to 44 understand circadian timekeeping in animals.

45

46 A fundamental challenge to addressing this guestion is the complexity of the circadian neuronal 47 networks. The paired mammalian SCN consist of tens of thousands of neurons with diverse 48 neurochemical outputs that form a complex network (reviewed by (7)). The clock neuron 49 network of Drosophila melanogaster offers a powerful model to understand the network 50 properties of neural circadian timekeeping. The molecular clocks of insects and mammals are 51 highly conserved and their neuronal networks appear to share common motifs (8). The fly's 52 clock neuron network consists of relatively few neurons that can be organized in a small number 53 of discrete anatomical classes ((9); Figure 1A). Furthermore, genetic tools to specifically 54 manipulate subclasses of the fly circadian network have made it possible to understand the 55 functional roles of these subclasses in the production of endogenous circadian rhythms in sleep 56 and activity (10, 11). Though transgenic markers of synaptic connectivity and live-imaging-57 based assessments of functional connectivity have been used to address neural connectivity

within the clock neuron network (e.g., (12, 13), a systematic assessment of synaptic connectivity
within this network is lacking.

60

61 The comprehensive mapping of synaptic connectivity using serial electron microscopy and 62 reconstruction of neuronal volumes allows to assess network structures of brain circuits (14). 63 Scheffer and colleagues (15) provided a dense reconstruction of chemical synapses within a 64 large portion of the fly's central brain, called the hemibrain. Annotation of the hemibrain 65 connectome contains most of the key anatomical subsets of the fly's clock neuron network and 66 powerful computational tools are available to navigate this connectome (15, 16) making it 67 possible to analyze the structure of the fly's brain clock network. 68 69 The Drosophila Circadian Neuron Network is a group of ~150 neurons that display synchronous 70 oscillation in PER and TIM abundance and can be subdivided based on gene expression, 71 anatomy, and location in the brain (17). These are (i) the lateral neurons (LNs), which can be 72 subdivided into ventral lateral (LNv) and dorsal lateral (LNd) neurons, (ii) the lateral posterior 73 neurons (LPNs), and (iii) the dorsal neurons (DNs), which can be subdivided into dorsal neurons 74 1, 2, and 3 (DN1, DN2, and DN3) and further subdivided into anterior (DN1a) and posterior

75 (DN1p) DN1s (9, 18, 19).

76

The LNvs release the key circadian neuropeptide Pigment Dispersing Factor (PDF) and can be
further subdivided into small and large LNvs (s-LNvs and I-LNvs). Release of PDF from the sLN_vs, which takes place in the dorsal protocerebrum where the LNds and DNs reside, is
required for endogenous circadian timekeeping (20, 21). The current annotation of the
hemibrain data set identifies all the expected lateral neuron classes: four I-LNvs, four s-LNvs,
the 5th-s-LNv, and six LNds ((15); Figure 1B and C). However, some clock neurons have not
yet been unequivocally identified within the hemibrain data set: approximately half of the DN1ps

(13, 15) and the DN2s and DN3s. The LN classes of clock neuron represent the minimum subnetwork required to produce endogenous bimodal rhythm of sleep and activity. A functional
molecular clock only in the s-LNvs, 5th-s-LNv, and LNds is sufficient to produce such rhythms
(22, 23).

88

89 Here we report an assessment of chemical synaptic connectivity for the critical LN clock neuron 90 classes within the hemibrain volume. We have determined the patterns of synaptic connectivity 91 within this core LN circadian sub-network and the connectivity with other clock neurons 92 annotated within the hemibrain dataset. This analysis provides significant and comprehensive 93 insight into the synaptic circuitry underlying the organization and function of the Drosophila 94 central brain clock. Our results reveal that previously identified anatomical and functional 95 subclasses of LNs are distinct connectomic classes which receive unique sources of synaptic 96 inputs and outputs. Furthermore, our analysis reveals a remarkable heterogeneity in how clock 97 neuron subclasses form connections to other clock neurons and identifies a small number of 98 clock cell subtypes that are highly synaptically coupled nodes. Finally, we find "non-clock 99 neuron" targets which themselves form synapses back onto clock neurons. We propose that 100 those non-clock cells are important components of the timekeeping network.

101

- 102 Results
- 103

104 The Clock Neuron Network and the Hemibrain Dataset

105

106 Representatives of all classes of clock neurons, with the exception of the DN2 and DN3 classes,

107 have been identified in the hemibrain volume used here (Figure 1A and B). See Table 1 for the

108 naming scheme used here for the clock neurons identified in the dataset with their

109 corresponding unique body IDs. The patterns of connectivity among some of these neurons 110 have recently been briefly described (11, 13). Scheffer and colleagues (15) define synaptic 111 strength within the hemibrain volume by the number of synaptic connections formed between 112 neurons, defining connections consisting of only one or two chemical synapses as weak and 113 subject to error, three to nine synapses as medium strength, and of ten or more synapses as 114 strong. We used these definitions of synaptic strength in this study. As a whole, the identified 115 clock neurons appear to be sparsely interconnected by chemical synapses. Most clock neuron 116 pairs form either no synapses or weak synaptic connections (Figure 1C). However, there are a few clear exceptions: a single LNd (LNd6) and the 5th s-LNv form strong connections with one 117 118 another and with members of the DN1 group (Figure 1C; see also Reinhard and colleagues 119 (13)) and stand out among the clock neurons as hubs of inter-clock synaptic connectivity.

120

121 To asses synaptic connectivity in the Drosophila clock network, we focused on three critical 122 classes of lateral clock neurons (LNs); the 4 Pigment Dispersing Factor (PDF) -expressing small 123 ventral lateral neurons (s-LNvs), the 6 dorsal lateral neurons (LNds) and the PDF negative 5th 124 s-LNv (Figure 1D). We have chosen to focus on these clock neuron classes for two reasons. 125 First, these classes are completely accounted for in the hemibrain annotation used here. 126 Second, the 11 neurons that comprise the LN class are sufficient to drive the fly's endogenous 127 bimodal rhythm in locomotor activity (22, 23) and therefore represent a critical sub-network 128 within the fly's circadian system.

129

130 The small LN_vs are a highly unified connectomic class distinct from the 5th s-LNv.

131

132 The s-LNvs have long been considered critical circadian pacemakers within the *Drosophila*

133 clock neuron network (24). These cells express the neuropeptide PDF (20, 25), maintain strong

134 molecular timekeeping under constant conditions (26, 27) and are required for robust

135 endogenous circadian rhythms (22, 28). The s-LNvs also contribute to the morning peak of the 136 fly's crepuscular daily activity rhythm (22, 29). Though by no means the only clock neurons 137 capable of producing an endogenous sense of time (30-32), a large body of evidence supports 138 the notion that s-LNvs are among the most critical neurons for the maintenance of endogenous 139 circadian rhythms (Reviewed by (11)). The 5th-s-LNv was named because it was initially thought 140 to be anatomically similar to the PDF positive s-LNvs in the larval brain (23, 33). However, subsequent work has suggested that the 5th s-LNv is likely functionally and anatomically more 141 142 akin to the LNds (22, 30, 34). 143 144 The four PDF-expressing s-LN_vs are characterized by a relatively simple morphology (Figure 145 2A-C; (19)). Their cell bodies are located in the ventral brain, near the accessory medulla 146 (AMe), into which they extend short neurites which likely receive input from photoreceptors (35, 147 36). These four s-LNvs project dorsally to the posterior dorsal protocerebrum, where they turn 148 toward the midline and form fine ramified termini that extend toward the midline (19, 37). These 149 dorsal ramifications are thought to be the major site of s-LNv synaptic output, but are also 150 known to contain synaptic inputs (38). Work by Schubert and colleagues (34) showed that the 151 5^{th} s-LNv (Fig 2F) has more extensive ramifications within the dorsal brain and accessory 152 medulla than the PDF expressing s-LNvs.

153

The four PDF-expressing s-LNvs and the 5th s-LNv have been identified within the hemibrain data set (Figures 1B-C and Figure 2A,F; (15)). Visualization of T-bars and postsynaptic densities within these neurons reveals that their ventral neurites, which innervate the AMe, are biased toward receiving synaptic input (Figure 2A and F). Individual PDF-positive s-LNvs display relatively simple dorsal medial termini with relatively few branch-points that tend to run in parallel to neighboring branches (Supplemental Figure 1). As previously described (38), these dorsal medial s-LNv termini contain both presynaptic and postsynaptic structures with the

161 former significantly outnumbering the latter (Figure 2A and Supplemental Figure 1). The dorsal termini of the 5th s-LNvs also contains both pre- and post-synaptic structures but appear to be 162 163 less biased toward output compared to the PDF expressing s-LNvs (Fig. 2F). Taken together, 164 the four pdf+ s-LNvs form a total of 2238 synapses within the hemibrain volume: 505 inputs 165 (postsynaptic densities) and 1733 outputs (projections onto postsynaptic densities). The single 5th s-LNv contains 1413 post-synaptic densities and forms synapses onto 1992 postsynaptic 166 167 densities. Thus, the 5th s-LNv forms about four times the number of synapses of a single PDF-168 positive s-LNv (Figure 4C: Supplemental Table S1 and S2).

169

170 The four *pdf*+ s-LNvs display uniformity in their synaptic inputs for strong synaptic connections. 171 Only three neurons in the hemibrain provide ten or more synapses onto at least one of these 172 cells (Figure 2D), and all four receive strong or medium strength synaptic inputs from these 173 three presynaptic cell types (Figure 4D; Supplemental Table S1). They also appear to be 174 remarkably uniform in their patterns of strong synaptic output. Only 11 neurons receive 10 or 175 more synapses from at least one pdf+ s-LNv (Figure 2E and 4E), and all 11 receive strong or 176 medium strength synapses from all four (Figure 4E; Supplemental Table S2). Compared to the 177 other LN classes, these s-LNvs are highly similar to each other in both their strong and medium 178 strength connections (Figure 4A and B) and form few but nearly uniform patterns of strong 179 shared synaptic connections (Figure 4D and E). Notably, within the hemibrain volume, the pdf+ 180 s-LNvs are not strongly connected to other clock neurons, though they do form medium strength connections with one another (Figures 1C and 2H). The 5th s-LNv displays patterns of strong 181 182 synaptic connectivity that are almost completely distinct from those of the four *pdf*+ s-LNvs, 183 sharing a single strong output connection with only one of these cells (Figure 2E).

184

Though quite uniform in their patterns of strong synaptic input and outputs, the *pdf*+ s-LNvs do
display some within-class differences in their patterns of weak and medium strength

187	connections. Among the inputs targeting only one s-LNv, and mediated by only three synapses,
188	is the HB-eyelet, a surprising finding given the long-held model that this external photoreceptor
189	provides direct excitatory input onto s-LN $_{\nu}$ s and contributes to light entrainment of circadian
190	rhythms (35, 36, 39), though recent work has indicated that the eyelet to s-LNv connection may
191	be polysynaptic (40). Nevertheless, our analysis supports the notion that the <i>pdf</i> + s-LN _v s
192	represent a uniform connectomic cell type with regard to patterns of strong synaptic
193	connections, consistent with recent work revealing a uniformity in gene expression across the s-
194	LNvs (41).
195	

196 The LNds comprise several connectomic subclasses.

197

198 As their name suggests, the somata of the dorsal lateral neurons (LNds) are situated dorsally 199 relative to the LNvs, residing in the lateral cell body rind (19, 33, 34). All six LNds send dorsal 200 medial projections across the superior protocerebrum and three send an additional projection 201 toward the ventral brain ((34); Figure 3A-C and Supplemental Figure S2). Though consisting of only two more neurons than the PDF-positive s-LNv class, the LNds form seven-times more 202 203 synaptic connections (6149 postsynaptic densities and projections to 9590 PSDs; compare 204 Figures 2A, 3A, and 4C) and are characterized by a much larger number of strong synaptic 205 partners. There are 164 distinct neurons that receive strong synaptic inputs from at least one 206 LNd (compared to 11 neurons for *pdf*+ s-LNvs; (Supplemental Table S2), and 86 distinct 207 neurons provide strong synaptic input onto at least one LNd (compared to three for s-LNvs; 208 Supplemental Table S2).

209

In addition to forming more synapses with more neurons than the PDF-positive s-LNvs, the
LNds are markedly less uniform in their patterns of strong synaptic connections (Figures 3E and
F and 4F and G). There is not a single source of strong synaptic input or a single neural target

213 of synaptic output that forms strong connections with all six LNds (Figure 3E and F. 214 Supplemental Tables S1 and S2). The maximum number of LNds that receive strong synaptic 215 inputs from the same presynaptic neuron is three (Figure 3F). The maximum number of LNds 216 that form strong synaptic outputs onto the same neuronal targets is also three (Figure 3F). 217 Based on these patterns of shared strong connectivity, there appear to be two connectomic 218 groups within the LNds, each consisting of three neurons: LNds 1-3 and LNds 4-6. LNds within 219 these two subgroups are more similar in their patterns of strong synaptic connectivity to each 220 other than to LNds of the other group (Figure 3E and F and 4F and G). These two groups differ 221 to a notable degree in the number of their synaptic connections, with the LNd 4-6 group forming 222 approximately twice the number of synaptic connections (Figure 4C: Supplemental Figure S2 223 and Supplemental Tables S1 and S2).

224

225 Examining the cellular morphology of the LNds within the hemibrain volume reveals that LNds 226 4-6 extend both dorsal-medial and ventral projections, whereas LNds 1-3 extend only dorsal-227 medial projections (Supplemental Figure S2). As shown by Schubert and colleagues (34), this 228 indicates that LNds 4-6 are the Cryptochrome (Cry) expressing LNds, while LNds 1-3 229 correspond to the Cry-negative LNds (Figure 3D). Though the Cry+ and Cry- subgroups of the 230 LNds appear to be two distinct connectomic subtypes, patterns of strong synaptic connectivity 231 suggest that the LNds can be further divided based on their patterns of strong synaptic 232 connections. Within the Cry+ LNds, LNd4 and LNd5 share 27 strong synaptic inputs with one 233 another, but only seven strong connections with LNd6 (Figure 3E). Similarly, LNd4 and LNd5 234 share 33 strong synaptic targets with one another but only seven or fewer with LNd6 (Figure 235 3F). Thus, the Cry+ LNds appear to consist of at least two connectomic subgroups, LNd4/LNd5 236 and LNd6. This connectomic distinction is consistent with differences in neuropeptide 237 expression within the Cry+ LNds, with two LNds expressing short neuropeptide F (sNPF) and 238 the third expressing ion transport peptide (ITP), a feature it shares with the Cry expressing 5th

s-LNv (42). A similar distinction can be made for the Cry-negative LNds, LNd2/LNd3 and LNd1,
in terms of patterns of strong synaptic connections (Figure 3E and F). Based on these patterns
of strong synaptic connections, the LNd class appears to consist of four distinct connectomic
types. This number matches the number of transcriptomic classes of LNds recently revealed by
single cell sequencing (41).

244

The four connectomic groups of LNd clock neurons correspond to previously identified
 cellular and functional clock subsets.

247

248 In addition to differences in *cry* expression, the LNds display other cellular and functional 249 distinctions, suggesting that this clock neuron class consists of multiple neuronal subtypes. The 250 LNds are divisible based on their expression of neuropeptides and neurotransmitters (42), with 251 two LNds co-expressing sNPF and Choline acetyltransferase (ChAT), an enzyme involved in 252 the biosynthesis of acetylcholine. Three LNds express Neuropeptide F (NPF), one of which 253 expresses a second peptide, ITP (42). The transmitter(s) produced by the remaining LNd are 254 not currently known. Furthermore, Cry+ and Cry- LNds differ in their expression of Pdf receptor 255 (PdfR), with the Cry+ LNds uniformly expressing PdfR and the Cry- LNds lacking receptor 256 expression (43), suggesting that these two groups of LNd are differentially sensitive to PDF 257 released from the I-LN_vs and s-LN_vs.

258

The coupling of LNds to circadian timekeeping within the s-LNvs varies among the LNds. The two sNPF positive LNds, which express Cry and PdfR, remain tightly coupled to the s-LNvs when the circadian clock in the latter neurons is slowed down (30). The sNPF expressing LNds were termed E1 oscillators based on this tight temporal coupling to the s-LNvs (30), which also express sNPF (42). The NPF/ITP expressing LNd, despite being receptive to PDF released from the LNvs, does not display coupling to the slowed s-LNv clocks and was grouped with the

ITP-expressing 5th s-LNv as E2 oscillators (30). The remaining LNds, which consist of the Cry
 negative LNds, were classified as E3 oscillators, which are neither PDF receptive nor coupled to
 s-LNvs with modified clock speeds (30).

268

269 The Cry+ LNds therefore appear to consist of two functional types; two LNds making up E1 and 270 a single LNd corresponding to E2. Schubert and colleagues (34) established the anatomical 271 hallmarks of these two Cry+ LNds, with the single E2 LNd sending more extensive ventral 272 projections compared to the E1 LNds. Examination of hemibrain LNd volumes indicates that 273 LNd6 corresponds to LNd-E2 (compare Supplemental Figure S2D and E to F), and that LNd4 274 and LNd5 are the E1 LNds. This LNd5/4 (E1) and LNd6 (E2) distinction mirrors the patterns of 275 shared strong synaptic connectivity displayed by the Cry+ LNds (Figure 3E and F). Therefore, 276 functionally distinct LNd subgroups share patterns of strong synaptic inputs and outputs.

277

The 5th s-LNv, which shares cellular and anatomical similarities with LNd6 (34, 42), was 278 279 assigned as a member of the E2 functional class by Yao and Shafer (30), based on the absence 280 of coupling to timekeeping within the PDF positive s-LNvs, despite receptivity to PDF and their role in the generation of evening activity (22). We therefore asked if LNd6 and the 5th s-LNv 281 282 display similar patterns of synaptic connectivity. Indeed, these two neurons displayed 283 significant overlap in their strong synaptic connectivity, both for synaptic inputs and targets (Figure 4F and G). Thus, LNd6 and the 5th s-LNv are more alike in their patterns of strong 284 285 synaptic connectivity than they are to other lateral neuron subtypes in addition to sharing 286 neuropeptide expression and coupling mode with the PDF expressing s-LNvs.

287

The patterns of strong clock neuron connectivity within the hemibrain led us to hypothesize that the recognized functional subtypes, M (PDF positive s-LNvs), E1 (LNd4 and LNd5), E2 (LNd6 and 5th s-LNv), and E3 (LNd1, LNd2, and LNd3) display distinct patterns of synaptic

291 connectivity. To test this hypothesis, we expanded our analysis to include both strong and 292 medium strength synaptic connections, which together account for the vast majority of 293 connections made by the identified clock neurons within the hemibrain dataset. To examine 294 affinities between individual identified clock neurons in our expanded consideration of 295 connectivity, we used the Jaccard index (Fig 4A and B), a coefficient of similarity between two 296 sets that ranges between zero and one, the former value indicating no overlapping synaptic 297 partners and latter indicating complete overlap (see methods). Jaccard indices for both synaptic 298 inputs (Fig 4A) and outputs (Fig 4B) provide strong evidence that the LN classes can be divided 299 into four connectomic groups: The four PDF positive s-LNvs (M group; Figure 6), two of the Crv+ LNds (LNd4 and LNd5; E1 group; Figure 7), LNd6 and the 5th s-LNv (E2 group; Figure 8 300 301 and Supplemental Figure S3), and the Cry-LNds (LNd1, LNd2, and LNd3; E3 Group; Figure 9), 302 conforming to the functional divisions hypothesized by Yao and Shafer (30).

303

304 These functional LN divisions also have different numbers of synaptic connections and different 305 ratios of input to output synapses. The M group displays the smallest number of synapses, E3 306 an intermediate number, and E1 and E2 form roughly twice the number of connections 307 displayed by E3 (Figure 4C). The M and E1 groups also appear distinct from the E2 and E3 308 groups in the balance of output to input synapses. Though all the identified LNs form more 309 synaptic outputs than inputs, output synapses in the M and E1 groups make up a larger 310 proportion of total synaptic connections when compared to the E2 and E3 groups (Figure 4). 311 Thus, the connectomic subgroups that emerged from our analysis of strong synaptic 312 connectivity (Figures 2-4) are further supported by the combined analysis of strong and medium 313 strength connectivity (Supplemental Figures 4 and 5) and conform to previously hypothesized 314 functional and cellular subgroups.

315

316 The Functional/Connectomic Subgroups of LN Clock Cells Display Distinct Synaptic

317 Output Pathways

318

319 In animals, the brain's endogenous central circadian clock drives myriad behavioral, 320 physiological, and endocrine rhythms. Synaptic connections between the central clock network 321 and neurons outside the timekeeping network are thought to mediate daily signals from the 322 circadian system to the neural centers responsible for driving daily physiological and behavioral 323 changes. Though specific output pathways linking the clock to specific endocrine and sleep 324 control centers have been previously described in the fly (Reviewed by (10, 44)), there is still a 325 great deal to be learned about circadian output signaling. For example, do the various functional 326 groups of clock neurons converge on the same synaptic targets to shape the timing of the same 327 daily outputs, as was recently described for arousal promoting pathways linking the LNs to 328 dopaminergic neurons modulating the ellipsoid body (45)? Alternatively, do functional clock cell 329 subgroups generally synapse onto distinct neural targets to produce uniquely phased outputs of 330 different behavioral, physiological, and endocrine rhythms, as recently described for sleep 331 modulating dorsal clock neurons (46, 47)? We examined the patterns of synaptic outputs of the 332 LN oscillator subgroups to determine how they coordinate the myriad circadian outputs.

333

334 As previously described (34) M, E1, E2, and E3 subgroups can be distinguished by their 335 patterns of neuropil innervation. As expected, the M, E1, E2, and E3 subgroups differ 336 significantly in terms of the brain areas where the majority of their neurites form chemical 337 synapses. Though the M and E subgroups form output synapses within both the superior lateral 338 protocerebrum (SLP) and superior medial protocerebrum (SMP), the M subgroups form the 339 majority of their output synapses within the SLP, whereas the E groups form the majority of their 340 output synapses within the SMP (Figure 5A and B). Though all seven E cells terminate largely 341 within these two neuropils, they fall, once again, into three classes with regard to their neuropil

innervation. For example, E1 forms more output synapses on cells of the anterior ventrolateral
protocerebrum (AVLP) than E2 or E3, E2 forms more synapses within the accessory medulla
(aMe) than do E1 or E3, and E3 forms little to no synapses on neurons associated with either of
these neuropils (Figure 5B).

346

347 The M subgroup's shared strong synaptic outputs represent only three distinct cell types (Figure 348 6). Among these are five neurons within the SLP, which represent only two cell-types: three 349 neurons annotated as SLP-316-R (Figure 6A) and two neurons annotated as SLP-403-R 350 (Figure 6B). The sixth strong shared output is an SMP-associated neuron named SMP232-R 351 (Figure 6C). The SLP-316-R neurons strongly resemble DN1ps currently missing from the 352 hemibrain annotation, which send ventral projections alongside the dorsal projections of M cells 353 and named ventral-contralateral DN1ps by Lamaze and colleagues (47) (Figure 6A and 354 Supplemental Figure S6). Jaccard indices support the conclusion that these strong shared 355 targets of M output are three distinct cell types (Figure 6D). Remarkably, all of the shared strong 356 output targets of the M group form synapses back onto identified clock neurons (Figure 6A-C), 357 including strong synaptic connections onto DN1ps and LPNs (Figure 6E). Thus, all the strong 358 and shared output targets of the M group project back to the clock neuron network, thereby 359 implicating them as nodes within the clock neuron network, either as currently unidentified 360 clock-containing neurons or non-clock-containing neurons. The M group appears to be unique in 361 the extent to which its strong shared synaptic targets reenter the clock neuron network, with 362 only half or fewer of strong E1, E2, or E3 targets recurring to the clock network in this fashion 363 (Figure 6F).

364

The E1 subgroup is characterized by many more strong/shared synaptic targets than the M subgroup (Compare Figure 4E and G) and these targets appear, based on Jaccard indices, to include many distinct cell types (Figure 7D). A minority of these E1 targets (16 out of 38) form

368 output synapses onto identified clock neurons within the hemibrain volume. Thus, the majority of 369 the strong shared synaptic outputs of E1 do not immediately project back to the clock neuron 370 network, in contrast to the uniform recurrence of strong shared M targets to the clock network 371 (Figure 6A-E). Several of the targets receiving the strongest E1 synaptic input do form strong 372 synaptic connections back onto clock neurons, particularly onto the E1 LNds themselves, in 373 addition to LPNs and DN1as (Figure 7E). Notably, the strong shared targets that recur to the 374 clock neuron network do not display the anatomical hallmarks of any of the currently 375 unannotated clock neurons in the hemibrain data set (e.g., Figure 7A-C). It therefore appears 376 that neurons that do not themselves possess molecular clocks might nevertheless reside within 377 the central timekeeping network and mediate polysynaptic connections between clock neurons. 378

379 The E2 subgroup, like E1, forms strong shared synapses on a much larger number of neuronal 380 targets than the M group (Compare Figure 4E and G) and these targets are a diverse array of 381 cell types. Approximately half (14 out of 26) of the strong and shared E2 targets form synaptic 382 connections onto identified clock neurons within the hemibrain (Figure 6F and 8A-C and E). 383 Compared to the recurrent E1 clock connections, E2 forms synapses on identified clock 384 neurons more broadly, forming connections with all currently identified clock neuron classes in 385 the hemibrain volume, with the exception of the DN1a class (Figure 8E). Thus, the E2 group 386 appears not only to represent a hub of strong direct inter-connectivity between identified clock 387 neuron classes (Figure 1C), but also provides additional synaptic clock network inputs via their 388 strong and shared synaptic targets (Figure 8E). As for E1, strong shared targets of E2 recurring 389 to the clock network include neurons that do not share obvious anatomical affinity for currently 390 unidentified clock neurons within the hemibrain dataset (e.g., Figure 8A-C). This suggests, once 391 again, that the circadian timekeeping network of Drosophila includes neurons that do not 392 themselves have a molecular clock.

393

394 Compared to the E1 and E2 groups, E3 forms approximately half the number of synaptic 395 connections (Figure 4C and G). With regard to its shared strong outputs, the E3 subgroup 396 forms strong shared synaptic connections onto only 16 neurons (Figure 3F and 4G), five of 397 which form synapses onto identified clock neurons within the hemibrain (Figure 9E). E3 outputs 398 onto clock neurons are limited to LNds and LPNs with most connections forming back onto E3 399 LNds themselves (Figure 9A-C and E). This makes E3 similar to the E1 group in that they are 400 characterized by strong shared output targets that form synapses directly back onto their E3 401 inputs (Figure 7E and Figure 9E). Once again, the strong and shared output targets recurring to 402 the clock network do not bear the anatomical hallmarks of clock neurons missing from the annotation (Figure 9A-C). 403

404

405 Taken together, our analysis indicates that the strong synaptic outputs of the four 406 functional/connectomic LN subgroups, M, E1, E2, and E3, diverge onto distinct neural targets 407 (Figure 4). Furthermore, many of these synaptic targets synapse back onto neurons within the 408 clock neuron network, including all of the shared and strong output targets of the M subgroup. 409 In contrast, approximately half of the synaptic targets of synaptic output from the E subgroups 410 do not immediately recur to the clock network (Figure 6F). Not only does this implicate specific 411 neuronal targets as conduits of circadian output, it also suggests that neurons not previously 412 identified as "clock neurons" represent integral nodes within the neural network from which 413 endogenous circadian timekeeping emerges (see discussion).

414

415 Discussion

416

417 The Clock Neuron Network within the Hemibrain Volume

419 Before discussing our connectomic analysis of the LN clock neuron classes, it is important to 420 acknowledge the limitations of the dataset. The hemibrain represents a single hemisphere of the 421 central brain and therefore does not contain all connections from the clock neuron cell bodies it 422 contains. Given that the clock neuron network is highly likely to contain connections between 423 contralateral neurons including clock neurons (48), our estimates of inter-clock connectivity will 424 therefore not include these contralateral connections. Furthermore, recent work suggests that 425 electrical synapses within the clock neuron network likely contribute to circadian timekeeping, 426 (49), but these are not visible in the hemibrain data set (15). Thus, our analysis underestimates 427 connectivity. In addition, clock neuron classes undergo pronounced daily morphological 428 changes that are most likely accompanied by changes in the number and locations of synaptic 429 connections (50-52). Thus, the hemibrain represents only one timepoint, within a cycle of 430 changing synaptic connections (15). Finally, the hemibrain data set represents a single female 431 fly, whereas the vast majority of experiments on the neural basis of circadian timekeeping have 432 employed male files. Thus, unexpected connectivity may be due to differences between the 433 well-characterized clock neuron network of males and the less well-studied female network.

434

435 Though we are focusing our analysis on the LN clock neuron classes, we have omitted the I-436 LNvs. We have done so because the synaptic outputs of the I-LNvs are thought to occur in the 437 contralateral accessory medulla (AMe) and much of their synaptic inputs are thought to located 438 in regions of the medulla that are not included in the hemibrain volume (48). We note, in this 439 context, that the I-LNvs do not appear to make significant contributions to endogenous circadian 440 timekeeping (26-28), which is the phenomenon we seek to illuminate here. Despite these 441 limitations, the organizational principles uncovered in this study provide insights into clock 442 network organization and are sure to generate a significant number of testable hypotheses 443 regarding network function (see below).

444

445 Connectomic Classes of LN Clock Neuron Mirror Previously Proposed Functional and

446 Molecular LN Sub-Groups

447

448 The lateral neuron classes are critical to maintain endogenous circadian rhythms (20, 24). An 449 examination of genetic mosaics suggested that, within the LNs, the PDF expressing LNvs drive the morning peak of daily activity, whereas PDF negative LNds and 5th s-LNv drive the evening 450 451 peak, leading to the designation of the former neurons as "Morning (M) Cells" and the latter as 452 "Evening (E) Cells" (22, 29). Though named based on its anatomical similarity to the other LNV 453 clock neurons in the larval brain (23, 33), there are now numerous observations suggesting that 454 the 5th-s-LNv is functionally and anatomically distinct from the PDF expressing s-LNvs in the 455 adult brain: the 4 pdf+ sLNvs are functionally associated with morning activity whereas the 5th-s-LNv is associated with evening activity (22). Furthermore the 5th s-LNv shares connectivity 456 457 patterns, neuropeptide expression, and features of cellular anatomy with one of the Cry-458 expressing LNds (30, 42, 53). Our connectomic analysis further supports the conclusion that the 5th s-LNv is an LNd-like clock neuron that bears little resemblance, functionally or anatomically, 459 460 to the PDF expressing s-LNvs.

461

462 Functional and anatomical analysis suggests that the LN neurons can be divided into four 463 functional classes, M, E1, E2, and E3 and that the patterns of strong connectivity displayed by 464 the LNs are in striking concordance with these divisions (30). Our connectomic analysis 465 indicates that the functional differences characterizing these four groups of neurons appear to 466 be written in the connectome: each receives a unique combination of strong synaptic inputs 467 and, in turn, forms strong synaptic connections onto distinct post-synaptic targets. These results 468 suggest that the functional subsets of LNs likely drive distinct behavioral and physiological 469 outputs, rather than converging onto the same premotor, sleep, or endocrine centers.

470

471 In addition, our analysis supports the existence of an additional subgroup within the LNs, 472 suggesting that the Cry- negative E3 class likely consists of two subgroups: LNd2 and LNd3, 473 which share a large proportion of their strong synaptic inputs and outputs, and LNd1, which 474 shares significantly fewer strong connections with the other two Cry- LNds (Figure 3E and F). 475 Placing LNd1 into its own LNd subgroup aligns our connectomic LN divisions with a recent 476 transcriptomic analysis of the clock neuron network that divided the LNds into four clusters: The 477 two sNPF and Cry expressing LNds (LNd4 and LNd5, i.e., E1), the single ITP and Cry 478 expressing LNd (LNd6, i.e. the E2 LNd), two NPF expressing LNds lacking Cry expression, and 479 a single Cry- LNd that lacks NPF (41). 480 481 The M group forms very few synaptic connections with other identified clock neuron 482 classes in the hemibrain dataset. 483 484 The s-LNvs of the M group, though they form medium strength connections with one another, 485 are almost completely isolated from the other identified clock neurons within the hemibrain 486 dataset (Figure 1C and 2H). Though this picture may ultimately underestimate of inter-clock connectivity if the strong shared SLP targets of M output (Figure 6A) are determined to be the 487 488 DN1ps currently missing from the annotation (Supplemental Figure S7). The predicted synaptic 489 inputs to the M group from the DN1ps (54-56) are not apparent in the hemibrain dataset, though 490 this may again be a limitation of the current annotation in which approximately half of the DN1ps 491 are unaccounted for. However, strong DN1p to s-LNv connections are lacking even if we 492 consider the three strong M cell targets, the SLP316s, to be missing DN1ps, as these form 493 synapses on DN1ps and LPNs, but not the M group (Supplemental Figure S7). Remarkably, 494 there are no synaptic connections between the M and E1 groups, the latter of which was 495 differentiated from E2 by the tight coupling of E1 molecular clocks to those of the M group (30). 496 Thus, the strong coupling of M and E1 likely takes place through non-synaptic connections,

497	consistent with recent work suggesting that the M group mediates its influence over
498	endogenous timekeeping via non-synaptic signaling mechanisms, most likely via the non-
499	synaptic release of PDF peptide (38, 50).
500	
501	Compared to the other LN subgroups, the M group forms the smallest number of synaptic

502 connections (Figure 4C). This group is also unique among the LN groups by virtue of the fact 503 that all of its shared strong synaptic output targets form strong synaptic connections onto clock 504 neurons (DN1ps and LPNs) (Figure 6E). Thus, the strongest synaptic outputs of the M groups 505 appear to be intimately associated with the clock neuron network, either as neurons directly 506 linking different clock neuron classes, or as currently unidentified clock neurons within the 507 hemibrain data set (see Supplemental Figure S7).

508

509 **The E1 and E2 groups are major conduits of synaptic output from the clock network.** 510

511 Compared to the other three LN functional groups, the E1 group forms the largest number of 512 connections onto post-synaptic neurons (Figures 3F and 4C) and the majority of their strong 513 and shared synaptic targets do not themselves form synapses onto identified clock neurons 514 within the hemibrain data set. Of the minority of strong shared E1 targets that do synapse onto 515 identified clock neurons, the majority form strong reciprocal connections with E1 itself (Figure 516 7E and 10A). Thus, the E group most strongly coupled with the critical M group (30) also 517 appears to be a major conduit of synaptic output from the clock neuron network.

518

Among the identified clock neurons within the hemibrain dataset, the E2 LNs (LNd6 and the 5th s-LNv) are clear outliers for synaptic connectivity with other clock neurons, forming strong synaptic connections onto E1 LNds and DN1ps. E2 LNds also receive strong synaptic inputs from DN1as and DN1ps and form strong connections with one another (Figure 1C). This strong

523 synaptic connectivity with other clock neurons may provide an explanation for the observation 524 that the E2 group fails to synchronize its molecular clock with the M group when the clocks of 525 the latter cells are slowed down, despite expressing the receptor for the M group's major 526 circadian output peptide PDF (30). Synaptic communication from non-M pacemakers may 527 prevent E2 clocks from synchronizing with those of the M cells. 528 529 Like the strong shared synaptic targets of E1 LNds, the majority of E2 strong output targets do 530 not synapse onto identified clock neurons. But, in contrast to E1, the minority of E2 targets that 531 do form strong connections with identified clock neurons do so more broadly than clock 532 recurrent E1 targets, forming strong synaptic connections onto the M group, E2, and the LPNs 533 (Figure 8E). Though not as numerous as the synaptic partners of E1, E2 forms many more 534 synaptic connections than either M or E3, and together E1 and E2 make up the bulk of synaptic 535 output from the LN classes (Figure 4C and Supplemental Table S2). Thus, there appear to be 536 two major circadian output conduits from the LN clock neurons within the hemibrain volume, one 537 of which is tightly coupled to the M group and the other whose output is likely more strongly 538 shaped by other clock neuron classes (30). 539 540 The E3 group is characterized by a pattern of strong synaptic output that is distinct from 541 E1 and E2 and is synaptically isolated from other identified clock neurons. 542 543 The E3 LNds are distinct from the E1 and E2 groups, in that they form approximately half the 544 number synaptic connections (Figure 4C). While clearly distinct from E1 and E2, the E3 group 545 displays some similarity to the M group with respect to its connectivity to identified clock 546 neurons in the hemibrain, forming very few connections with other clock classes while being 547 interconnected by medium strength connections (Figure 1C). Among the identified clock 548 neurons in the hemibrain, the strong output targets of E3 make strong reciprocal connections

back to E3, but not to other identified clock neuron classes, though they do form a few medium
strength connections onto LPNs (Figure 9E). This sets E3 clearly apart from the other LN
groups, all of which have strong synaptic targets that form strong synapses onto other clock
neuron classes (Compare Figures 6E, 7E, 8E, and 9E). Thus, the E3 group appears to be
uniquely isolated from other identified clock neuron classes for both direct and indirect synaptic
connectivity.

555

556 The E3 group is unique among the LN clock neurons by virtue of its lacking CRY and PdfR 557 expression (43, 57) and is therefore thought to be relatively isolated from both light/dark cycles 558 (58) and PDF released from the LNvs. Indeed, the E3 group entrains its molecular clocks more 559 readily to environmental temperature cycles than to light cycles (58) and does not synchronize 560 with PDF expressing LNvs with slowed clocks (30). A close examination of E3 output pathways 561 and the extent to which they converge or fail to converge on endocrine, sleep, and pre-motor 562 centers will offer important insights into how light and temperature are integrated by the 563 circadian system to entrain to environmental cycles of both light and temperature, the latter of 564 which lag behind the former in natural environments.

565

566 Neurons without endogenous molecular clocks are likely integral to the central circadian
 567 pacemaker network.

568

The LN clock neuron classes are critical nodes of circadian timekeeping and are predicted to communicate directly with endocrine, sleep, and pre-motor centers to drive circadian outputs (10, 44) and with other clock neuron classes to coordinate network timekeeping (Reviewed by (11)). Thus, the LN classes are assumed to synapse upon other clock neurons to promote an endogenous sense of time and upon non-clock neurons to mediate daily changes in physiology

and behavior. Our analysis reveals the presence of a third type of LN clock output target,
neurons that mediate connections between identified clock neurons (e.g., Figure 10B and C).

577 All four functional classes of LN (M, E1, E2, and E3) provide strong synaptic outputs onto 578 neurons that, in turn, form strong synaptic connections onto identified clock neurons within the 579 hemibrain volume (Figures 6E and F, 7E, 8E, and 9E). In the case of E1 and E3 much of the 580 strong output recurring to the clock neuron network is reciprocal. For example, the strong 581 targets of E1 outputs preferentially form strong connections back onto E1 LNds (Figure 7E). For 582 all four groups of LN, strong outputs recurring to the clock network form either strong or medium strength synapses on the LPNs, implicating this class as a particularly rich hub for polysynaptic 583 584 inter-clock connectivity (Figures 6E, 7E, 8E, 9E, and 10C; (13)).

585

Most of the neurons forming strong but indirect connections between identified clock neurons bear no resemblance to known clock neurons and are unlikely therefore to express the molecular circadian clock (e.g., Figure 10B and C). This finding suggests the need to expand our conception of what constitutes the fly's circadian clock network to include "non-clock" neurons that provide strong synaptic connections between the neurons with endogenous molecular circadian clocks (Figure 10D). What role might such "inter-clock-neurons" play within a circadian network? Networks underlying central pattern generators (CPGs) might offer clues.

594 Many CPG networks consist of neurons both with and without endogenous pacemaking activity 595 (Reviewed by (59)). In such networks, connections between pacemaker neurons and follower 596 neurons profoundly shape the time-course of rhythmic outputs, increase the precision of the 597 central pattern generator, and provide a means for adjusting the phasing of its outputs (e.g., 598 (60-63)). Given the distributed daily phases of neural activity displayed by the various classes 599 of clock neurons (64), the circadian pace-making network represents a central pattern

600	generator, albeit a lumberingly slow one. We hypothesize that the "inter-clock neurons" we've
601	identified here (e.g., Figure 10 B and C) play significant roles in the determination of the
602	circadian system's endogenous period, precision, and phasing of rhythmic outputs, much like
603	the follower neurons of central pattern generators described above.
604	
605	This testable hypothesis is just one of many that emerge from the comprehensive view of clock
606	connectomics afforded by the hemibrain data set (15). This remarkable picture of the synaptic
607	connectivity displayed by clock neurons identified in this data set (Supplemental Tables 1 and
608	2), in conjunction with the open-source neuro-informatic resources available to the field (e.g.,
609	(16)) and the highly specific genetic tools available for the manipulation of identified neurons
610	(e.g., (65)), will be the basis of a great deal of future work on the neural basis of circadian
611	entrainment, timekeeping, and output.
612	
613	Methods
613 614	Methods Connectome Data and Neuron Identification
614	
614 615	Connectome Data and Neuron Identification
614 615 616	Connectome Data and Neuron Identification All of the data analyzed in this study come from the Hemibrain v1.2.1 dataset made publicly
614 615 616 617	Connectome Data and Neuron Identification All of the data analyzed in this study come from the Hemibrain v1.2.1 dataset made publicly available by Janelia Research Campus (15). The data details a full connectome derived from
614 615 616 617 618	Connectome Data and Neuron Identification All of the data analyzed in this study come from the Hemibrain v1.2.1 dataset made publicly available by Janelia Research Campus (15). The data details a full connectome derived from EM sections of a significant portion of the right hemisphere of a female <i>Drosophila</i> brain and
614 615 616 617 618 619	Connectome Data and Neuron Identification All of the data analyzed in this study come from the Hemibrain v1.2.1 dataset made publicly available by Janelia Research Campus (15). The data details a full connectome derived from EM sections of a significant portion of the right hemisphere of a female <i>Drosophila</i> brain and small portions of the left hemisphere. These data were collected from a wild type female brain
614 615 616 617 618 619 620	Connectome Data and Neuron Identification All of the data analyzed in this study come from the Hemibrain v1.2.1 dataset made publicly available by Janelia Research Campus (15). The data details a full connectome derived from EM sections of a significant portion of the right hemisphere of a female <i>Drosophila</i> brain and small portions of the left hemisphere. These data were collected from a wild type female brain reared under a 12-hour light, 12-hour dark cycle. The specimen was dissected at 5 days of age,

623 Hemibrain data was accessed via neuPrint and Fly Brain Observatory. Visualization of

624 morphological data was done in the Fly Brain Observatory web interface (NeuroNLP.Hemibrain)

625 while the retrieval of connectome data was done with the Neuprint python package

626 (https://github.com/connectome-neuprint/neuprint-python). Analyses were aided by the use of

627 the pandas (<u>https://pandas.pydata.org/</u>), seaborn (<u>https://seaborn.pydata.org/</u>), and superVenn

- 628 (https://github.com/gecko984/supervenn) python packages.
- 629

630 Each neuron in the database has a unique bodyID number and may also be identified with a 631 cell-type name based on the name it was given in the literature or on its location and anatomy. 632 Clock neurons were identified in the database from gueries based on their known cell-type 633 names. This means that there may be clock neurons that have been traced in the hemibrain, but 634 if Janelia had not labeled them with their known cell name within the annotation, we have not 635 included them as clock neurons here. The bodyID numbers for identified clock neurons were 636 collected and used in the connectivity analyses to ensure consistency between platforms and 637 future annotations.

638

The full table of clock neurons, their unique body IDs, and their sequential labels are provided below. The hemibrain annotation does not sequentially label instances of the same cell type. The Fly Brain Observatory does sequentially label cell type instances, however, there is no guarantee that the sequential labeling will consistently correspond to the specific body IDs. Thus, we employed a sequential labeling on a single retrieval from FBO and have used this labeling consistently throughout the paper (Table 1).

645

646 **Table 1: Identification of Clock Neurons within the Hemibrain Volume**

bodyld	type	Sequential label	subphase
2068801704	s-LNv	s-LNv1	М
1664980698	s-LNv	s-LNv2	М
2007068523	s-LNv	s-LNv3	М

1975347348	s-LNv	s-LNv4	М
5813056917	LNd	LNd4	E1
5813021192	LNd	LNd5	E1
5813069648	LNd	LNd6	E2
511051477	5th s-LNv	5th s-LNv	E2
296544364	LNd	LNd1	E3
448260940	LNd	LNd2	E3
5813064789	LNd	LNd3	E3
356818551	LPN	LPN1	
480029788	LPN	LPN2	
450034902	LPN	LPN3	
546977514	LPN	LPN4	
264083994	DN1a	DN1a1	
5813022274	DN1a	DN1a2	
5813010153	DN1pA	DN1pA1	
324846570	DN1pA	DN1pA2	
325529237	DN1pA	DN1pA3	
387944118	DN1pA	DN1pA4	
387166379	DN1pA	DN1pA5	
386834269	DN1pB	DN1pB1	
5813071319	DN1pB	DN1pB2	
1884625521	I-LNv	ILNv1	
2065745704	I-LNv	ILNv2	
5813001741	I-LNv	ILNv3	
5813026773	I-LNv	ILNv4	

647

648

649 Morphological Data Visualization with FlyBrainLab

650

FlyBrainLab (16) is available as a python environment and a user-friendly web interface. The

652 platform displays the hemibrain EM data and enables the analysis of the connectome data. The

653 morphology images in our paper were generated in FlyBrainLab.

654 Connectivity Analysis

Synaptic connectivity data were retrieved from the Janelia hemibrain dataset. Our analyses included the synapses to or from traced but unnamed fragments as well as select orphan bodies, in addition to synapses from full, traced, and named neurons. Fragments are partial or truncated neurons that mainly lie beyond or at the boundaries of the hemibrain section. Although fragments were often unidentified cell types, we felt their inclusion was warranted to obtain as accurate a picture as possible of the relative amounts of synaptic connectivity to and from clock neurons.

662

In keeping with Scheffer and colleagues (15), the synaptic strengths reported in our paper correspond to the number of postsynaptic densities counted on the postsynaptic neuron that are abutted by the presynaptic T-bar sites from the presynaptic neuron in question. Polyadic synapses, where a single presynaptic T-bar site contacts multiple postsynaptic sites, are common in the Drosophila brain (15, 66). Thus, synaptic weight for both the presynaptic and postsynaptic neuron is quantified as the postsynaptic density count.

669

We adopted the criteria from Scheffer *et. al* (15) to categorize connectivity strength. A weak connection is defined as a synaptic connection weight less than three. A medium strength connection is between three and nine synapses, while a strong connection is a strength equal to or greater than ten synapses. In our study, these criteria are applied to the total synapse count (i.e. the total number of postsynaptic densities) between two neurons rather than to the per-ROI synapse counts between them. Wherever applicable, the connection strength criteria used for any analysis or visualization is stated in the figure legend and in the main text.

677

The Sankey figures are based only on strong synaptic connections. Connectivity data were retrieved using the criteria for strong connections and exported into tables. The network structure of the clock connectome was graphed using the synaptic connectivity data retrieved from the hemibrain data and the networkX python package (https://networkx.org). Nodes are individual clock neurons and edges are labeled with the total synaptic connection weights from one neuron to another.

684 Jaccard Indices

685 The Jaccard similarity coefficient is defined as the ratio of the intersection and the union of two 686 sets.

$$687 J(A, B) = \frac{A \cap B}{A \cup B}$$

688

In the context of our study the Jaccard index represents the amount of overlap among the synaptic partners of two neurons. The Jaccard index is a number between 0 and 1, with 0 indicating no overlap and with 1 indicating that the sets of synaptic partners for two neurons are identical.

693 Availability of Analysis Code

694

The data retrieval routines and the analyses used in this paper were done in the python coding language. We have made our scripts publicly available upon request in a GitHub repository.

698

699 Acknowledgements:

701 This work was supported by grants from the National Institute of Neurological Disorders and Stroke R01NS077933 to O.T.S. and R01NS118012 to M.P.F. and O.T.S., start-up funds from 702 703 Barnard College (M.P.F.) and the State of New York (O.T.S.), grants NIH K22 NS104187, NSF 704 NeuroNex Award DBI-1707398, and The Gatsby Charitable Foundation to G.J.G, and Barnard 705 SRI funds to K.L and A.M. We are grateful to Larry Abbot, Annika Barber and Michael Rosbash 706 for helpful discussions and to Larry Abbot, Justin Blau, Abhilash Lakshman, Ashok Litwin-Kumar 707 Paul Taghert, Aishwarya Ramakrishnan and Robert Veline for kindly providing comments on the 708 manuscript. Figures 1A and 10A were created in Biorender. 709 710

- 711 Figure Legends:
- 712
- 713
- 714 Main Figures
- 715

716 Figure 1. The circadian clock neuron network and identified clock neurons in the 717 hemibrain. (A) The circadian clock network is shown in both hemispheres. Currently identified 718 cells are shown in color (s-LNvs red, I-LNvs light red, LNds in orange, DN1a in purple, a subset 719 of DN1p in blue) and known clock cells not yet identified within the hemibrain connectome data 720 are shown in gray (DN2, DN3, and a subset of DN1p). The pars intercerebralis (PI) and optic 721 lobe (OL) are indicated in gray. (B) Identified clock neurons in the hemibrain. Neuropils are 722 shown in gray. Color codes as indicated in (A). (C) Heatmap indicates synaptic connections 723 strength among all identified circadian clock neurons, including weak (weight <3) connections. 724 (D) The timekeeping lateral neurons that compose the morning (M) and evening (E) Oscillators: s-LNvs (M cells), and 5th s-LNv and LNds (E cells). 725

726

727 Figure 2. Connectivity patterns of the s-LNvs. (A-C). Synaptic connections of the four pdf+ s-728 LNvs, s-LNv R 1 through s-LNv R 4. Neuronal morphology is shown in gray. In A and B, 729 inputs to the s-LNvs are shown in blue, outputs are shown in magenta. (A) All connections, 730 including non-clock cells, (B) Connections to/from clock cells only, excluding connections to s-731 LNvs, (C) Connections among the 4 pdf+ s-LNvs. Input and output sides coincide and are 732 indicated in green. (D-E) Sankey diagram indicating the strong synaptic partners of all s-LNvs, including the 5th s-LNv. The total weight of synapses formed by each cell with its inputs (D) or 733 734 outputs (E) is shown. (D) Presynaptic partners (inputs) of s-LNvs. No shared connections were 735 found between the pdf+ s-LNvs and the 5th s-LNv. (E) Post synaptic partners (outputs) of s-LNvs. Only one cell (Body ID 571372889) receives synaptic input from the 5th s-LNv plus a *pdf*+ 736

s-LNv. (F-G) Synaptic connections of the 5th s-LNv. (F) All connections, including non-clock
cells, (G) Connections to clock cells only. (H) Connectivity map of the four *pdf*+ s-LNvs.

739

740 Figure 3. Connectivity patterns of the LNds. (A-C). Synaptic connections of the six LNds. 741 Neuronal morphology is shown in gray. In A and B, inputs to the s-LNvs are shown in blue, 742 outputs are shown in magenta. (A) All connections, including non-clock cells, (B) Connections to 743 clock cells only, excluding connections to LNds. Input and output sides coincide and are 744 indicated in green. (C) Connections within LNds. (D) Connectivity map of the six LNds. (E-F) 745 Sankey diagram indicating the strong synaptic partners of all LNds. The total weight of 746 synapses formed by each cell with its inputs (E) or outputs (F) is shown. (E) Pre-synaptic 747 partners of LNds. No shared connections were found between LNd1-3 and LNd4-6. Most of the 748 shared connections are between LNd4 and LNd5 (X cells provide strong inputs to both). (F) 749 Post synaptic partners of the LNds.

750

751 Figure 4. M cells are homogeneous while E cells can be clustered in three distinct

752 groups. (A-B) Jaccard indices for overlap in synaptic partners of M and E cells. Only includes 753 synaptic partners that make medium or strong connections. Higher index values indicate more 754 similarity in either inputs (A) or outputs (B). (C) Total input and output Synapse counts for M and 755 E cells. (D-E) Strong shared connections of the four *pdf*+ s-LNvs. Only cells that share one 756 connection with at least two M cells are shown. The strength (weight) of the connection is 757 indicated. Only medium and strong connections are included. (D) The two cells that send strong 758 connections to at least two M cells send strong connections to all 4. (E) The six cells that 759 receive strong connections from at least two M cells receive strong connections from all 4. (F-G) Strong shared connections of the six LNds plus the 5th s-LNv (collectively referred to as E cells). 760 761 Only cells that share a strong connection with at least two E cells are shown. The strength 762 (weight) of the connection is indicated. Only medium and strong connections are included. (F) 763 Cells that send strong connections to at least two E cells are included in the heatmap. (G) Cells 764 that receive strong connections from at least two E cells are included in the heatmap.

765

Figure 5. Neuropils innervated by M and E cells. (A-B). Percentage of connections located in
each of the indicated neuropils. Medium and strong connections are included. (A) Neuropils in
which the outputs of each of the 4 *pdf*+ s-LNvs are located. (B) Neuropils in which the outputs of
each of the LNds and the 5th s-LNv are located.

770

771 Figure 6. Strong shared outputs of M cells. (A-C) The six cells that are strong shared outputs 772 of the four M cells involve three different neuronal types (SPL316-R, SLP403-R, and SMP232-773 R). The M cells outputs onto each representative neuron of each type are shown in magenta. 774 Representative target neurons are shown in green. (A) M cells contact three SPL316 neurons. 775 Left, all four M cells are shown in gray and their contacts to 355453590 (neuronal morphology 776 shown in green) are shown in magenta. Right: 355453590 is shown in gray and its outputs to 777 clock cells are shown in magenta. (B) M cells contact two SPL403-R neurons. Left, all four M 778 cells are shown in gray and their contacts to 325455002 (neuronal morphology shown in green) are shown in magenta. Right: 325455002 is shown in gray and its outputs to clock cells are 779 780 shown in magenta. (C) M cells contact one SMP232-R neuron. Left, all four M cells are shown

781 in gray and their contacts to 325455002 (neuronal morphology shown in green) are shown in 782 magenta. Right: 325455002 is shown in gray and its outputs to clock cells are shown in 783 magenta. (D) Jaccard index of the six M cell shared output cells. The index is based on the 784 similarity of their outputs, the more similar their outputs are the higher the index value. Y and x-785 axis indicate the cell body ID of each of the six cells. Their neuronal type is indicated to the left 786 of the body ID on the y axis. Only indices >=0.01 are shown. (E) All strong shared outputs of M 787 cells in turn contact clock neurons. On the x-axis, the clock neurons that receive contacts from 788 each cell are indicated. The values on the cells represent the weight of each connection. 789 Medium and strong connections are included. (F) Percent of strong shared outputs of each 790 neuronal class that in turn sends contacts to clock cells. Medium and strong connections are 791 included. E1 = LNd4 and LNd5, E2 = LNd6 and the 5th s-LNv, E3= LNd1, LNd2 and LNd3. 792

793 Figure 7. Strong shared outputs of E1. (A-C) The cells that are strong shared outputs of E1 794 involve multiple neuronal types. E1 outputs onto three representative neurons are shown. E1 795 neurons (LNd4 and LNd5) are shown in gray in the left panels, where representative output 796 neurons are shown in green. On the right panels, each representative cell is shown in gray and its contacts to clock cells are shown in magenta (A) E1 cells contact two SMP368-R neurons. 797 798 Left, E1 neurons (shown in gray) contacts to SMP368-R neuron 390331583 (shown in green) 799 are shown in magenta. (B) E1 cells contact two AVLP075-R neurons. Left, E1 neurons (shown 800 in gray) contacts to AVLP075-R neuron 702152113 (shown in green) are shown in magenta. (C) 801 E1 cells contact two SMP315-R neurons. Left, E1 neurons (shown in gray) contacts to SMP315-802 R neuron 5813040712 (shown in green) are shown in magenta. (D) Jaccard indices indicating 803 overlap among the output synaptic partners of the top 10 E1 strong shared output cells. The 804 index is based on the similarity of their outputs, the more similar their outputs are the higher the 805 index value. Y and x-axis indicate the cell body ID of each of the six cells. Only indices >=0.01 806 are shown. (E) Most shared outputs of E1 cells that contact clock cells send strong contacts to 807 both E1 neurons. On the x-axis, the clock neurons that receive contacts from each cell are 808 indicated. The values on the cells represent the weight of each connection. Medium and strong 809 connections are included.

810

811 Figure 8. Strong shared outputs of E2. (A-C) The cells that are strong shared outputs of E2 812 involve multiple neuronal types. E2 outputs onto three representative neurons are shown. E2 813 neurons (LNd6 and the 5th s-LNv) are shown in gray in the left panels, where representative 814 output neurons are shown in green. On the right panels, each representative cell is shown in 815 gray and its contacts to clock cells, if present, are shown in magenta (A) Left, E2 neurons 816 (shown in gray) contacts to SMP368 neuron 329732855 (shown in green) are shown in 817 magenta. (B) Left, E2 neurons (shown in gray) contacts to SLP249 neuron 356140100 (shown 818 in green) are shown in magenta. (C) Left, E2 neurons (shown in gray) contacts to aMe22 819 neuron 5813021192 (shown in green) are shown in magenta. (D) Jaccard indices for the 820 outputs of the top 10 E2 strong shared output cells. The index is based on the similarity of their 821 outputs, the more similar their outputs are the higher the index value. Y and x-axis indicate the 822 cell body ID of each of the ten cells. One of the strong shared outputs of E2 is LNd4. Only 823 indices >=0.01 are shown. (E) Shared outputs of E2 that contact clock cells contact different 824 clock subclasses. On the x-axis, the clock neurons that receive contacts from each cell are

indicated. The values on the cells represent the weight of each connection. Medium and strongconnections are included.

827

828 Figure 9. Strong shared outputs of E3. (A-C) The cells that are strong shared outputs of E3 829 involve multiple neuronal types. E3 outputs onto three representative neurons are shown. E3 830 neurons (LNd1, LNd2, and LNd3) are shown in gray in the left panels, where representative 831 output neurons are shown in green. On the right panels, each representative cell is shown in 832 gray and its contacts to clock cells are shown in magenta. (A) Left, E3 neurons (shown in gray) 833 contacts to SMP335 neuron 297243542 (shown in green) are shown in magenta. (B) Left, E3 834 neurons (shown in gray) contacts to SMP486 neuron 327933679 (shown in green) are shown in 835 magenta. (C) Left, E3 neurons (shown in gray) contacts to SMP334 neuron 360254108 (shown 836 in green) are shown in magenta. (D) Jaccard indices for the outputs of the top 11 E3 strong 837 shared output cells. The index is based on the similarity of their outputs, the more similar their 838 outputs are the higher the index value. Y and x-axis indicate the cell body ID of each of the 839 cells, Only 3 cells are strong shared outputs of all E3 cells (E3a+ E3b), 8 cells are strong shared 840 targets of E3a only. Only indices >=0.01 are shown. (E) Shared outputs of any two E3 cells that 841 contact clock cells. On the x-axis, the clock neurons that receive contacts from each cell are 842 indicated. The values on the cells represent the weight of each connection. Medium and strong connections are included. 843

844

845 Figure 10. Connections within the clock neuron network. (A) Combined weights of medium 846 and strong connections among different classes of identified clock neurons. Arrows indicate the 847 direction of the connection. Some classes, such as E2, are strongly interconnected, while other 848 clusters are relatively isolated. (B) Representative strong shared output of E1 that in turn 849 contacts clock neurons. E1 are indicated in gray, their strong shared target LHPV6m1 cell 850 388881226 is indicated in green, and its strong target neurons DNa1 and 2 are indicated in 851 magenta (the weight of output contacts is 19 and 10, respectively). (C) Representative strong 852 shared output of E2 that in turn contacts clock neurons. E2 are indicated in gray, their strong 853 shared target SMP223 cell 417143726 is indicated in green, and its strong target neurons LPN 854 are indicated in magenta (the weight of output contacts is 14 to LPN, 18 to LPN2, and 20 to 855 LPN3). (D) Summary of 'inter-clock' neurons providing strong poly synaptic connections 856 between clock neurons.

857 858

859 Supplementary Figures

860

Supplementary Figure 1. Connections of individual s-LNvs. (A-D). Synaptic connections of each of the four *pdf*+ s-LNvs, s-LNv1 (A), s-LNv2 (B), s-LNv3 (C) and s-LNv4 (D), either to all neurons (left columns), to other clock cells except s-LNvs (middle columns), or to other s-LNvs (right columns). Neuronal morphology is shown in gray. Inputs to the s-LNvs are shown in blue, outputs are shown in magenta. Body IDs of each s-LNv are indicated on the right.

867 **Supplementary Figure 2. Connections of individual LNds**. (A-F). Synaptic connections of 868 each of the six LNds, LNd1 (A), LNd2 (B), LNd3 (C), LNd4 (D), LNd5 (E) and LNd6 (F) either to

all neurons (left columns), to other clock cells except LNds (middle columns), or to other LNds
(right columns). Neuronal morphology is shown in gray. Inputs to the LNds are shown in blue,
outputs of the LNds are shown in magenta. Body IDs of each LNd are indicated on the right.

872

Supplementary Figure 3. Connections of E cell classes. (A-C). Synaptic connections of the three E cell classes, E3a (A), E1 (B), and E2 (C) either to all neurons (left columns), to other clock cells except LNds (middle columns), or to other LNds (right columns). LNd1 alone (E3b) is shown in Suppl. Figure 2A. Neuronal morphology is shown in gray. Inputs to the E classes are shown in blue, outputs are shown in magenta (left and middle columns). Within each group (right columns), input and output sides coincide and are indicated in green.

879

Supplementary Figure 4. Comparison of medium and strong inputs of 5th s-LNv relative 880 to the pdf+ s-LNvs and the LNds. (A-B) Supervenn diagrams indicate the number of shared 881 inputs between all combinations of neurons, either among the 5th s-LNv and the LNds (A) or 882 among the 5th s-LNv and the *pdf*+ s-LNvs (B). Each neuron is represented in a row, boxes in 883 884 color indicate inputs to that neuron. The numbers on the right y-axis indicate the total number of 885 neurons that provide input to that cell. For example, 74 neurons provide medium and strong 886 inputs to LNd3. The numbers on the x-axis indicate the number of shared inputs between 887 different combinations of cells.

888

Supplementary Figure 5. Comparison of medium and strong outputs of 5th s-LNv relative 889 to the pdf+ s-LNvs and the LNds. (A-B) Supervenn diagrams indicate the number of shared 890 891 outputs between all combinations of neurons, either among the 5th s-LNv and the LNds (A) or among the 5th s-LNv and the *pdf*+ s-LNvs (B). Each neuron is represented in a row, boxes in 892 color indicate inputs to that neuron. The numbers on the right y-axis indicate the total number of 893 894 neurons that are being contacted by a specific cell. For example, 172 neurons receive medium 895 or strong contacts from LNd3. The numbers on the x-axis indicate the number of shared outputs 896 between different combinations of cells.

897

Supplementary Figure 6. Connections of individual strong shared outputs of s-LNvs. (AF). Synaptic connections of each of the six cells that receive strong shared inputs from all four *pdf*+ s-LNvs. Each cell is indicated in gray. Inputs from clock neurons to each cell are indicated
in blue, and outputs from each cell to any clock neurons are indicated in magenta. (A-C) Three
SLP316 receive the strongest contacts from all *pdf*+ s-LNvs and are indicated in gray. (D-E)
Two SLP403 are indicated in gray. (F) SMP223 is indicated in gray.

904

Supplementary Figure 7. Neuroanatomy of the three SLP316 cells and identified DN1s.
(A) Five DN1ps (green) that exhibit contralateral as well as dorsal projections have been identified, and are referred to as DN1pA. (B) Two DN1ps (magenta) that lack a contralateral or dorsal projection but extend ventrally and medially have been identified and are referred to as DN1pB. (C) The three SPL316 neurons (gray) have both dorsal and ventral projections and a short medial projection. (D) Overlap of DN1pA, DN1pB, and SLP316.

- 911
- 912

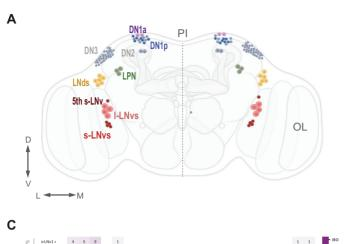
913 References

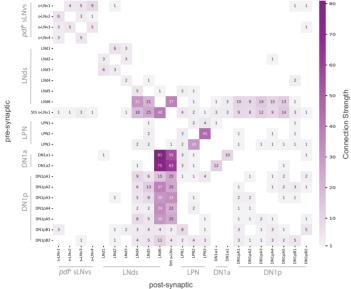
915	1.	J. Aschoff, Handbook of behavioral neurobiology, biological rhythms (Plenum Press,
916 917	2	New York, ed. 4, 1981). J. S. Takahashi, Turek, F.W., Moore, R.Y., <i>Biological Rhythms</i> , Handbook of Behavioral
917 918	2.	Neurobiology (Plenum Press, New York, ed. 12, 2001).
918 919	3.	E. D. Herzog, Neurons and networks in daily rhythms. <i>Nat Rev Neurosci</i> 8, 790-802
920	5.	(2007).
921	4.	E. D. Herzog, T. Hermanstyne, N. J. Smyllie, M. H. Hastings, Regulating the
922	т.	Suprachiasmatic Nucleus (SCN) Circadian Clockwork: Interplay between Cell-
923		Autonomous and Circuit-Level Mechanisms. Cold Spring Harb Perspect Biol 9 (2017).
924	5.	A. C. Liu <i>et al.</i> , Intercellular coupling confers robustness against mutations in the SCN
925	0.	circadian clock network. <i>Cell</i> 129 , 605-616 (2007).
926	6.	E. D. Buhr, S. H. Yoo, J. S. Takahashi, Temperature as a universal resetting cue for
927	0.	mammalian circadian oscillators. <i>Science</i> 330 , 379-385 (2010).
928	7.	M. H. Hastings, E. S. Maywood, M. Brancaccio, The Mammalian Circadian Timing
929		System and the Suprachiasmatic Nucleus as Its Pacemaker. <i>Biology (Basel)</i> 8 (2019).
930	8.	M. N. Nitabach, P. H. Taghert, Organization of the Drosophila circadian control circuit.
931		<i>Curr Biol</i> 18 , R84-93 (2008).
932	9.	O. T. Shafer, C. Helfrich-Forster, S. C. Renn, P. H. Taghert, Reevaluation of Drosophila
933		melanogaster's neuronal circadian pacemakers reveals new neuronal classes. J Comp
934		Neurol 498 , 180-193 (2006).
935	10.	O. T. Shafer, A. C. Keene, The Regulation of Drosophila Sleep. Curr Biol 31, R38-R49
936		(2021).
937	11.	M. Ahmad, W. Li, D. Top, Integration of Circadian Clock Information in the Drosophila
938		Circadian Neuronal Network. J Biol Rhythms 36, 203-220 (2021).
939	12.	Z. Yao, A. M. Macara, K. R. Lelito, T. Y. Minosyan, O. T. Shafer, Analysis of functional
940		neuronal connectivity in the Drosophila brain. Journal of neurophysiology 108, 684-696
941		(2012).
942	13.	N. Reinhard et al., The lateral posterior clock neurons of Drosophila melanogaster
943		express three neuropeptides and have multiple connections within the circadian clock
944		network and beyond. J Comp Neurol 10.1002/cne.25294 (2021).
945	14.	N. Kasthuri <i>et al.</i> , Saturated Reconstruction of a Volume of Neocortex. <i>Cell</i> 162 , 648-661
946		(2015).
947	15.	L. K. Scheffer <i>et al.</i> , A connectome and analysis of the adult Drosophila central brain.
948	40	Elife 9 (2020).
949	16.	A. A. Lazar, T. Liu, M. K. Turkcan, Y. Zhou, Accelerating with FlyBrainLab the discovery
950 054		of the functional logic of the Drosophila brain in the connectomic and synaptomic era.
951 052	17	<i>Elife</i> 10 (2021). C. Helfrich-Forster, Neurobiology of the fruit fly's circadian clock. <i>Genes Brain Behav</i> 4 ,
952 953	17.	
953 954	18.	65-76 (2005). C. Helfrich-Forster <i>et al.</i> , The lateral and dorsal neurons of Drosophila melanogaster:
954 955	10.	new insights about their morphology and function. Cold Spring Harb Symp Quant Biol
955 956		72 , 517-525 (2007).
957	19.	C. Helfrich-Forster <i>et al.</i> , Development and morphology of the clock-gene-expressing
958	13.	lateral neurons of Drosophila melanogaster. J Comp Neurol 500 , 47-70 (2007).
959	20.	S. C. Renn, J. H. Park, M. Rosbash, J. C. Hall, P. H. Taghert, A pdf neuropeptide gene
960	20.	mutation and ablation of PDF neurons each cause severe abnormalities of behavioral
961		circadian rhythms in Drosophila. <i>Cell</i> 99 , 791-802 (1999).
		,

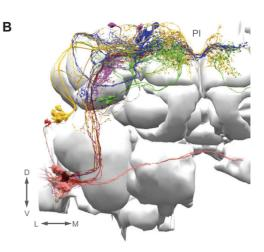
962	21.	J. H. Park et al., Differential regulation of circadian pacemaker output by separate clock
962 963	21.	genes in Drosophila. Proc Natl Acad Sci U S A 97 , 3608-3613 (2000).
964	22.	B. Grima, E. Chelot, R. Xia, F. Rouyer, Morning and evening peaks of activity rely on
965		different clock neurons of the Drosophila brain. Nature 431, 869-873 (2004).
966	23.	D. Rieger, O. T. Shafer, K. Tomioka, C. Helfrich-Forster, Functional analysis of circadian
967		pacemaker neurons in Drosophila melanogaster. J Neurosci 26, 2531-2543 (2006).
968	24.	C. Helfrich-Forster, Robust circadian rhythmicity of Drosophila melanogaster requires
969		the presence of lateral neurons: a brain-behavioral study of disconnected mutants. J
970	05	Comp Physiol A 182 , 435-453 (1998).
971	25.	C. Helfrich-Forster, The period clock gene is expressed in central nervous system
972 973		neurons which also produce a neuropeptide that reveals the projections of circadian pacemaker cells within the brain of Drosophila melanogaster. <i>Proc Natl Acad Sci U S A</i>
973 974		92 , 612-616 (1995).
975	26.	Z. Yang, A. Sehgal, Role of molecular oscillations in generating behavioral rhythms in
976	20.	Drosophila. <i>Neuron</i> 29 , 453-467 (2001).
977	27.	O. T. Shafer, M. Rosbash, J. W. Truman, Sequential nuclear accumulation of the clock
978		proteins period and timeless in the pacemaker neurons of Drosophila melanogaster. J
979		Neurosci 22 , 5946-5954 (2002).
980	28.	O. T. Shafer, P. H. Taghert, RNA-interference knockdown of Drosophila pigment
981		dispersing factor in neuronal subsets: the anatomical basis of a neuropeptide's circadian
982		functions. <i>PLoS One</i> 4 , e8298 (2009).
983	29.	D. Stoleru, Y. Peng, J. Agosto, M. Rosbash, Coupled oscillators control morning and
984	~~	evening locomotor behaviour of Drosophila. Nature 431 , 862-868 (2004).
985	30.	Z. Yao, O. T. Shafer, The Drosophila circadian clock is a variably coupled network of
986	24	multiple peptidergic units. <i>Science</i> 343 , 1516-1520 (2014).
987 988	31.	M. Schlichting, M. M. Diaz, J. Xin, M. Rosbash, Neuron-specific knockouts indicate the importance of network communication to Drosophila rhythmicity. <i>Elife</i> 8 (2019).
989 989	32.	R. Delventhal <i>et al.</i> , Dissection of central clock function in Drosophila through cell-
990	02.	specific CRISPR-mediated clock gene disruption. <i>Elife</i> 8 (2019).
991	33.	M. Kaneko, J. C. Hall, Neuroanatomy of cells expressing clock genes in Drosophila:
992		transgenic manipulation of the period and timeless genes to mark the perikarya of
993		circadian pacemaker neurons and their projections. J Comp Neurol 422, 66-94 (2000).
994	34.	F. K. Schubert, N. Hagedorn, T. Yoshii, C. Helfrich-Forster, D. Rieger, Neuroanatomical
995		details of the lateral neurons of Drosophila melanogaster support their functional role in
996		the circadian system. <i>J Comp Neurol</i> 526 , 1209-1231 (2018).
997	35.	S. Malpel, A. Klarsfeld, F. Rouyer, Larval optic nerve and adult extra-retinal
998		photoreceptors sequentially associate with clock neurons during Drosophila brain
999	20	development. <i>Development</i> 129 , 1443-1453 (2002).
1000	36.	C. Helfrich-Forster <i>et al.</i> , The extraretinal eyelet of Drosophila: development,
1001 1002	27	ultrastructure, and putative circadian function. <i>J Neurosci</i> 22 , 9255-9266 (2002).
1002	37.	C. Helfrich-Förster, Development of pigment-dispersing hormone-immunoreactive neurons in the nervous system of Drosophila melanogaster. <i>Journal of Comparative</i>
1003		Neurology 380, 335-354 (1997).
1005	38.	K. Yasuyama, I. A. Meinertzhagen, Synaptic connections of PDF-immunoreactive lateral
1006	00.	neurons projecting to the dorsal protocerebrum of Drosophila melanogaster. <i>J Comp</i>
1007		Neurol 518 , 292-304 (2010).
1008	39.	D. Rieger, R. Stanewsky, C. Helfrich-Forster, Cryptochrome, compound eyes, Hofbauer-
1009		Buchner eyelets, and ocelli play different roles in the entrainment and masking pathway
1010		of the locomotor activity rhythm in the fruit fly Drosophila melanogaster. J Biol Rhythms
1011		18 , 377-391 (2003).

 M. T. Li <i>et al.</i>, Hub-organized parallel circuits of central circadian pacemaker neurons for visual photoentrainmen in Drosophila. <i>Nat Commun</i> 9, 4247 (2018). D. Ma <i>et al.</i>, A transcriptomic taxonomy of Drosophila circadian neurons around the clock. <i>Elife</i> 10 (2021). H. A. D. Johard <i>et al.</i>, Peptidergic clock neurons in Drosophila: Ion transport peptide and short neuropeptide F in subsets of dorsal and ventral lateral neurons. <i>The Journal of Comparative Neurology</i> 516, 59-73 (2009). S. H. Im, W. Li, P. H. Taghert, PDFR and CRY signaling converge in a subset of clock neurons to modulate the amplitude and phase of circadian behavior in Drosophila. <i>PLoS One</i> 6, e18974 (2011). A. N. King, A. Sehgal, Molecular and circuit mechanisms mediating circadian clock output in the Drosophila brain. <i>Eur J Neurosci</i> 51, 268-281 (2020). K. Liang <i>et al.</i>, Morning and Evening Circadian Pacemakers Independently Drive Premotor Centers via a Specific Dopamine Relay. <i>Neuron</i> 102, 843-857 e844 (2019). F. Guo, M. Holla, M. Diaz, M. Rosbash, A Circadian Output Circuit Controls Sleep-Wake Arousal in Drosophila. <i>Neuron</i> 100, 624-635 e624 (2018). A. Lamaze, P. Kratschmer, K. F. Chen, S. Lowe, J. E. C. Jepson, A Wake-Promoting Circadian Output Circuit in Drosophila. <i>Curt Biol</i> 28, 3098-3105 e3093 (2018). C. Hefirch-Forster <i>et al.</i>, The lateral and dorsal neurons of Drosophila melanogaster: new insights about their morphology and function. <i>Cold Spring Harb Symp Quant Biol</i> 72, 517-525 (2007). A. Ramakrishnan, V. Sheeba, Gap junction protein Innexin2 modulates the period of free-running hythms in Drosophila melanogaster. <i>IScience</i> 24, 103011 (2021). M. D. Harant <i>et al.</i>, Circadian Structural Plasticity Drives Remodeling of neuronal circuits involved in rhythmic behavior. <i>PLoS Biol</i> 6, e69 (2008). J. M. Duhart <i>et al.</i>, Circadian Neuron 1964, S08 (2020). B. J.			
 D. Ma[*] <i>et al.</i>, A transcriptomic taxonomy of Drosophila circadian neurons around the clock. <i>Elife</i> 10 (2021). H. A. D. Johard <i>et al.</i>, Peptidergic clock neurons in Drosophila: Ion transport peptide and short neuropeptide F in subsets of dorsal and ventral lateral neurons. <i>The Journal of Comparative Neurology</i> 516, 59-73 (2009). S. H. Im, W. Li, P. H. Taghert, PDFR and CRY signaling converge in a subset of clock neurons to modulate the amplitude and phase of circadian behavior in Drosophila. <i>PLoS One</i> 6, e18974 (2011). A. N. King, A. Sehgal, Molecular and circuit mechanisms mediating circadian clock output in the Drosophila brain. <i>Eur J Neurosci</i> 51, 268-281 (2020). X. Liang <i>et al.</i>, Morning and Evening Circadian Pacemakers Independently Drive Premotor Centers via a Specific Dopamine Relay. <i>Neuron</i> 102, 843-857 e844 (2019). F. Guo, M. Holla, M. M. Diaz, M. Rosbash, A Circadian Output Circuit Controls Sleep-Wake Arousal in Drosophila. <i>Neuron</i> 100, 624-635 e624 (2018). A. Lamaze, P. Kratschmer, K. F. Chen, S. Lowe, J. E. C. Jepson, A Wake-Promoting Circadian Output Circuit in Drosophila. <i>Curr Biol</i> 28, 3098-3105 e3093 (2018). C. Helfrich-Forster <i>et al.</i>, The lateral and dorsal neurons of Drosophila melanogaster: new insights about their morphology and function. <i>Cold Spring Harb Symp Quant Biol</i> 72, 517-525 (2007). M. P. Fernandez, J. Berni, M. F. Ceriani, Circadian neuronal circuits involved in rhythmic behavior. <i>PLoS Biol</i> 6, e68 (2008). M. P. Fernandez, J. Berni, M. F. Ceriani, Circadian neuronal incrusit. <i>Curr Biol</i> 30, 504-5048 e5045 (2020). J. M. Duhart <i>et al.</i>, Circadian Structural Plasticity Drives Remodeling of neuronal circuits involved in rhythmic behavior. <i>PLoS Biol</i> 6, e68 (2008). J. M. Duhart <i>et al.</i>, Circadian clock neurons constantly monitor environmental temperature to set sleep timing. <i>Nature</i> 555, 98		40.	•
 clock. <i>Elife</i> 10 (2021).¹ H. A. D. Johard <i>et al.</i>, Peptidergic clock neurons in Drosophila: Ion transport peptide and short neuropeptide F in subsets of dorsal and ventral lateral neurons. <i>The Journal of</i> <i>Comparative Neurology</i> 516, 59-73 (2009). S. H. Im, W. Li, P. H. Taghert, PDFR and CRY signaling converge in a subset of clock neurons to modulate the amplitude and phase of circadian behavior in Drosophila. <i>PLoS</i> <i>One</i> 6, e18974 (2011). A. N. King, A. Sehgal, Molecular and circuit mechanisms mediating circadian clock output in the Drosophila brain. <i>Eur J Neurosci</i> 51, 268-281 (2020). X. Liang <i>et al.</i>, Morning and Evening Circadian Pacemakers Independently Drive Premotor Centers via a Specific Dopamine Relay. <i>Neuron</i> 102, 843-857 e844 (2019). F. Guo, M. Holla, M. M. Diaz, M. Rosbash, A Circadian Output Circuit Controls Sleep- Wake Arousal in Drosophila. <i>Neuron</i> 100, 624-635 e624 (2018). A. Lamaze, P. Kratschmer, K. F. Chen, S. Lowe, J. E. C. Jepson, A Wake-Promoting Circadian Output Circuit in Drosophila. <i>Neuron</i> 100, 803-903 (2018). C. Helfrich-Forster <i>et al.</i>, The lateral and dorsal neurons of Drosophila melanogaster: new insights about their morphology and function. <i>Cold Spring Harb Symp Quant Biol</i> 72, 517-525 (2007). A. Ramakrishnan, V. Sheeba, Gap junction protein Innexin2 modulates the period of free-running rhythms in Drosophila melanogaster. <i>Science</i> 24, 103011 (2021). M. P. Fernandez, J. Berni, M. F. Ceriani, Circadian remodeling of neuronal circuits involved in rhythmic behavior. <i>PLoS Biol</i> 6, e69 (2008). J. M. Duhart <i>et al.</i>, Circadian Structural Plasticity Drives Remodeling of E Cell Output. <i>Curr Biol</i> 30, 5040-5048 e5045 (2020). S. Yadlapall <i>et al.</i>, Circadian Circadian constantly monitor environmental temperature to set sleep timing. <i>Nature</i> 555, 98-102 (2018). S. Yadlapall <i>et al.</i>, Circadian Clock neurons constantly monitor environmental temperature to set sl			
 42. H. A. D. Johard <i>et al.</i>, Peptidergic clock neurons in Drosophila: Ion transport peptide and short neuropeptide F in subsets of dorsal and ventral lateral neurons. <i>The Journal of</i> <i>Comparative Neurology</i> 516, 59-73 (2009). 43. S. H. Im, W. Li, P. H. Taghert, PDFR and CRY signaling converge in a subset of clock neurons to modulate the amplitude and phase of circadian behavior in Drosophila. <i>PLoS</i> <i>One</i> 6, e18974 (2011). 44. A. N. King, A. Sehgal, Molecular and circuit mechanisms mediating circadian clock output in the Drosophila brain. <i>Eur J Neurosci</i> 51, 268-281 (2020). 45. X. Liang <i>et al.</i>, Morning and Evening Circadian Pacemakers Independently Drive Premotor Centers via a Specific Dopamine Relay. <i>Neuron</i> 102, 843-857 e844 (2019). 46. F. Guo, M. Holla, M. M. Diaz, M. Rosbash, A Circadian Output Circuit Controls Sleep- Wake Arousal in Drosophila. <i>Neuron</i> 100, 624-635 e624 (2018). 47. A. Lamaze, P. Kratschmer, K. F. Chen, S. Lowe, J. E. C. Jepson, A Wake-Promoting Circadian Output Circuit in Drosophila. <i>Curr Biol</i> 28, 3098-3105 e3093 (2018). 48. C. Helfrich-Forster <i>et al.</i>, The lateral and dorsal neurons of Drosophila melanogaster: new insights about their morphology and function. <i>Cold Spring Harb Symp Quant Biol</i> 72, 517-525 (2007). 49. A. Ramakrishnan, V. Sheeba, Gap junction protein Innexin2 modulates the period of free-running rhythms in Drosophila melanogaster. <i>iScience</i> 24, 103011 (2021). 50. M. P. Fernandez, J. Berni, M. F. Ceriani, Circadian remodeling of neuronal circuits involved in rhythmic behavior. <i>PLoS Biol</i> 6, e69 (2008). 51. J. M. Duhart <i>et al.</i>, Circadian Structural Plasticity Drives Remodeling of E Cell Output. <i>Curr Biol</i> 30, 5040-5048 e5045 (2020). 52. B. J. Song, S. J. Sharp, D. Rogulja, Daily rewiring of a neural circuit generates a predictive model of environmental light. <i>Sci AdvT</i> (2021). 54. F. Guo <i>et al.</i>, Circadian		41.	
 short neuropeptide F in subsets of dorsal and ventral lateral neurons. <i>The Journal of Comparative Neurology</i> 516, 59-73 (2009). S. H. Im, W. Li, P. H. Taghert, PDFR and CRY signaling converge in a subset of clock neurons to modulate the amplitude and phase of circadian behavior in Drosophila. <i>PLoS One</i> 6, e18974 (2011). A. N. King, A. Sehgal, Molecular and circuit mechanisms mediating circadian clock output in the Drosophila brain. <i>Eur J Neurosci</i> 51, 268-281 (2020). X. Liang <i>et al.</i>, Morning and Evening Circadian Pacemakers Independently Drive Premotor Centers via a Specific Dopamine Relay. <i>Neuron</i> 102, 843-857 e844 (2019). F. Guo, M. Holla, M. M. Diaz, M. Rosbash, A Circadian Output Circuit Controls Sleep-Wake Arousal in Drosophila. <i>Neuron</i> 100, 624-635 e624 (2018). A. Lamaze, P. Kratschmer, K. F. Chen, S. Lowe, J. E. C. Jepson, A Wake-Promoting Circadian Output Circuit in Corosophila. <i>Curr Biol</i> 28, 3098-3105 e3093 (2018). C. Helfrich-Forster <i>et al.</i>, The lateral and dorsal neurons of Drosophila melanogaster: new insights about their morphology and function. <i>Cold Spring Harb Symp Quant Biol</i> 72, 517-525 (2007). M. P. Fernandez, J. Berni, M. F. Ceriani, Circadian Structural Patrib Symp Quant Biol 72, 517-525 (2007). M. P. Fernandez, J. Berni, M. F. Ceriani, Circadian remodeling of neuronal circuits involved in rhythmic behavior. <i>PLoS Biol</i> 6, e69 (2008). J. M. Duhart <i>et al.</i>, Circadian Structural Plasticity Drives Remodeling of E Cell Output. <i>Curr Biol</i> 30, 5040-5048 e5045 (2020). B. J. Song, S. J. Sharp, D. Rogulja, Daily rewiring of a neural circuit generates a predictive model of environmental light. <i>Sci Adv</i> 7 (2021). X. Liang, T. E. Holy, P. H. Taghert, A Series of Suppressive Signals within the Drosophila Circadian Neural Circuit Generates Sequential Daily Outputs. <i>Neuron</i> 94, 1173-1189 e11774 (2017). F. Guo <i>et al.</i>, Circadian neuron feedback controls the Drosophila sleep			
 Comparative Neurology 516, 59-73 (2009). S. H. Im, W. Li, P. H. Taghert, PDFR and CRY signaling converge in a subset of clock neurons to modulate the amplitude and phase of circadian behavior in Drosophila. <i>PLoS One</i> 6, e18974 (2011). A. N. King, A. Sehgal, Molecular and circuit mechanisms mediating circadian clock output in the Drosophila brain. <i>Eur J Neurosci</i> 51, 268-281 (2020). X. Liang <i>et al.</i>, Morning and Evening Circadian Pacemakers Independently Drive Premotor Centers via a Specific Dopamine Relay. <i>Neuron</i> 102, 843-857 e844 (2019). F. Guo, M. Holla, M. M. Diaz, M. Rosbash, A Circadian Output Circuit Controls Sleep-Wake Arousal in Drosophila. <i>Neuron</i> 100, 624-635 e624 (2018). A. Lamaze, P. Kratschmer, K. F. Chen, S. Lowe, J. E. C. Jepson, A. Wake-Promoting Circadian Output Circuit in Drosophila. <i>Curr Biol</i> 28, 3098-3105 e3093 (2018). C. Helfrich-Forster <i>et al.</i>, The lateral and dorsal neurons of Drosophila melanogaster: new insights about their morphology and function. <i>Cold Spring Harb Symp Quant Biol</i> 72, 517-525 (2007). A. Ramakrishnan, V. Sheeba, Gap junction protein Innexin2 modulates the period of free-running rhythms in Drosophila melanogaster. <i>Iscience</i> 24, 103011 (2021). M. P. Fernandez, J. Berni, M. F. Ceriani, Circadian remodeling of neuronal circuits involved in rhythmic behavior. <i>PLoS Biol</i> 6, e69 (2008). J. M. Duhart <i>et al.</i>, Circadian Structural Plasticity Drives Remodeling of E Cell Output. <i>Curr Biol</i> 30, 5040-5048 e5045 (2020). S. X. Liang, T. E. Holy, P. H. Taghert, A Series of Suppressive Signals within the Drosophila Circadian Neural Circuit Generates Sequential Daily Outputs. <i>Neuron</i> 94, 1173-1189 e1174 (2017). K. Liang, T. E. Holy, P. H. Taghert, A Series of Suppressive Signals within the Drosophila Circadian Neural Circuit Generates Sequential Daily Outputs. <i>Neuron</i> 94, 1173-1189 e1174 (2017). F. Guo et		42.	
 S. H. Im, W. Li, P. H. Taghert, PDFR and CRY signaling converge in a subset of clock neurons to modulate the amplitude and phase of circadian behavior in Drosophila. <i>PLoS</i> <i>One</i> 6, e18974 (2011). A. N. King, A. Sehgal, Molecular and circuit mechanisms mediating circadian clock output in the Drosophila brain. <i>Eur J Neurosci</i> 51, 268-281 (2020). X. Liang <i>et al.</i>, Morning and Evening Circadian Pacemakers Independently Drive Premotor Centers via a Specific Dopamine Relay. <i>Neuron</i> 102, 843-857 e844 (2019). F. Guo, M. Holla, M. M. Diaz, M. Rosbash, A Circadian Output Circuit Controls Sleep- Wake Arousal in Drosophila. <i>Neuron</i> 100, 624-635 e624 (2018). A. Lamaze, P. Kratschmer, K. F. Chen, S. Lowe, J. E. C. Jepson, A Wake-Promoting Circadian Output Circuit in Drosophila. <i>Curr Biol</i> 28, 3098-3105 e3093 (2018). C. Helfrich-Forster <i>et al.</i>, The lateral and dorsal neurons of Drosophila melanogaster: new insights about their morphology and function. <i>Cold Spring Harb Symp Quant Biol</i> 72, 517-525 (2007). A. Ramakrishnan, V. Sheeba, Gap junction protein Innexin2 modulates the period of free-running rhythms in Drosophila melanogaster. <i>Science</i> 24, 103011 (2021). M. P. Fernandez, J. Berni, M. F. Ceriani, Circadian remodeling of neuronal circuits involved in rhythmic behavior. <i>PLoS Biol</i> 6, e69 (2008). J. M. Duhart <i>et al.</i>, Circadian Structural Plasticity Drives Remodeling of E Cell Output. <i>Curr Biol</i> 30, 5040-5048 e5045 (2020). B. J. Song, S. J. Sharp, D. Rogulja, Daily rewiring of a neural circuit generates a predictive model of environmental light. <i>Sci Adv</i> 7 (2021). X. Liang, T. E. Holy, P. H. Taghert, A Series of Suppressive Signals within the Drosophila Circadian neuron feedback controls the Drosophila sleepactivity profile. <i>Nature</i> 536, 292-297 (2016). F. Guo <i>et al.</i>, Circadian clock neurons constantly monitor environmental temperature to set sleep tim			• •
 neurons to modulate the amplitude and phase of Circadian behavior in Drosophila. <i>PLoS</i> 00re 6, e18974 (2011). A. N. King, A. Sehgal, Molecular and circuit mechanisms mediating circadian clock output in the Drosophila brain. <i>Eur J Neurosci</i> 51, 268-281 (2020). X. Liang et al., Morning and Evening Circadian Pacemakers Independently Drive Premotor Centers via a Specific Dopamine Relay. <i>Neuron</i> 102, 843-857 e844 (2019). F. Guo, M. Holla, M. M. Diaz, M. Rosbash, A Circadian Output Circuit Controls Sleep-Wake Arousal in Drosophila. <i>Neuron</i> 100, 624-635 e624 (2018). A. Lamaze, P. Kratschmer, K. F. Chen, S. Lowe, J. E. C. Jepson, A Wake-Promoting Circadian Output Circuit in Drosophila. <i>Curr Biol</i> 28, 3098-3105 e3093 (2018). C. Helfrich-Forster <i>et al.</i>, The Iateral and dorsal neurons of Drosophila melanogaster: new insights about their morphology and function. <i>Cold Spring Harb Symp Quant Biol</i> 72, 517-525 (2007). A. Ramakrishnan, V. Sheeba, Gap junction protein Innexin2 modulates the period of free-running rhythms in Drosophila melanogaster. <i>iScience</i> 24, 103011 (2021). M. P. Fernandez, J. Berni, M. F. Ceriani, Circadian remodeling of neuronal circuits involved in rhythmic behavior. <i>PLoS Biol</i> 6, e69 (2008). J. M. Duhart <i>et al.</i>, Circadian Structural Plasticity Drives Remodeling of E Cell Output. <i>Curr Biol</i> 30, 5040-5048 e5045 (2020). S. J. Song, S. J. Sharp, D. Rogulja, Daily rewiring of a neural circuit generates a predictive model of environmental light. <i>Sci Adv</i> 7 (2021). K. Liang T. E. Holy, P. H. Taghert, A Series of Suppressive Signals within the Drosophila et al., Circadian clock neurons constantly monitor environmental temperature to set Jeep timing. <i>Naur</i> 655, 98-102 (2018). F. Guo <i>et al.</i>, Circadian clock neurons constantly monitor environmental temperature to set Jeep timing. <i>Nauw</i> 555, 98-102 (2018). F. Guo <i>et al.</i>, Circadian			
 One 6, e18974 (2011). A. N. King, A. Sehgal, Molecular and circuit mechanisms mediating circadian clock output in the Drosophila brain. <i>Eur J Neurosci</i> 51, 268-281 (2020). X. Liang <i>et al.</i>, Morning and Evening Circadian Pacemakers Independently Drive Premotor Centers via a Specific Dopamine Relay. <i>Neuron</i> 102, 843-857 e844 (2019). F. Guo, M. Holla, M. M. Diaz, M. Rosbash, A Circadian Output Circuit Controls Sleep-Wake Arousal in Drosophila. <i>Neuron</i> 100, 624-635 e624 (2018). A. Lamaze, P. Kratschmer, K. F. Chen, S. Lowe, J. E. C. Jepson, A Wake-Promoting Circadian Output Circuit Control Sophila. <i>Neuron</i> 100, 624-635 e624 (2018). A. Lamaze, P. Kratschmer, K. F. Chen, S. Lowe, J. E. C. Jepson, A Wake-Promoting Circadian Output Circuit in Torsophila. <i>Neuron</i> 1801 28, 3098-3105 e3093 (2018). C. Helfrich-Forster <i>et al.</i>, The lateral and dorsal neurons of Drosophila melanogaster: new insights about their morphology and function. <i>Cold Spring Harb Symp Quant Biol</i> 72, 517-525 (2007). A. Ramakrishnan, V. Sheeba, Gap junction protein Innexin2 modulates the period of free-running rhythms in Drosophila melanogaster. <i>IScience</i> 24, 103011 (2021). M. P. Fernandez, J. Berni, M. F. Ceriani, Circadian remodeling of neuronal circuits involved in rhythmic behavior. <i>PLoS Biol</i> 6, e69 (2008). J. M. Duhart <i>et al.</i>, Circadian Structural Plasticity Drives Remodeling of E Cell Output. <i>Curr Biol</i> 30, 5040-5048 e5045 (2020). S. J. Song, S. J. Sharp, D. Rogulja, Daily rewiring of a neural circuit generates a predictive model of environmental light. <i>Sci Adv 7</i> (2021). X. Liang, T. E. Holy, P. H. Taghert, A Series of Suppressive Signals within the Drosophila Circadian neuron feedback controls the Drosophila sleepactivity profile. <i>Nature</i> 536, 292-297 (2016). S. Yadlapalli <i>et al.</i>, Circadian clock neurons constantly monitor environmental temperature to set slee		43.	
 A. N. King, A. Sehgal, Molecular and circuit mechanisms mediating circadian clock output in the Drosophila brain. <i>Eur J Neurosci</i> 51, 268-281 (2020). X. Liang et al., Morning and Evening Circadian Pacemakers Independently Drive Premotor Centers via a Specific Dopamine Relay. <i>Neuron</i> 102, 843-857 e844 (2019). F. Guo, M. Holla, M. M. Diaz, M. Rosbash, A Circadian Output Circuit Controls Sleep- Wake Arousal in Drosophila. <i>Neuron</i> 100, 624-635 e624 (2018). A. Lamaze, P. Kratschmer, K. F. Chen, S. Lowe, J. E. C. Jepson, A Wake-Promoting Circadian Output Circuit in Drosophila. <i>Curr Biol</i> 28, 3098-3105 e3093 (2018). C. Helfrich-Forste <i>et al.</i>, The lateral and dorsal neurons of Drosophila melanogaster: new insights about their morphology and function. <i>Cold Spring Harb Symp Quant Biol</i> 72, 517-525 (2007). A. Ramakrishnan, V. Sheeba, Gap junction protein Innexin2 modulates the period of free-running rhythms in Drosophila melanogaster. <i>iScience</i> 24, 103011 (2021). M. P. Fernandez, J. Berni, M. F. Ceriani, Circadian remodeling of neuronal circuits involved in rhythmic behavior. <i>PLoS Biol</i> 6, e69 (2008). J. M. Duhart <i>et al.</i>, Circadian Structural Plasticity Drives Remodeling of E Cell Output. <i>Curr Biol</i> 30, 5040-5048 e5045 (2020). S. J. Song, S. J. Sharp, D. Rogulja, Daily rewiring of a neural circuit generates a predictive model of environmental light. <i>Sci Adv</i> 7 (2021). X. Liang, T. E. Holy, P. H. Taghert, A Series of Suppressive Signals within the Drosophila Circadian Neural Circuit Generates Sequential Daily Outputs. <i>Neuron</i> 94, 1173-1188 e1174 (2017). F. Guo <i>et al.</i>, Circadian neuron feedback controls the Drosophila sleepactivity profile. <i>Nature</i> 536, 292-297 (2016). S. Yadlapalli <i>et al.</i>, Sites of Circadian Clock Neuron Plasticity Mediate Sensory Integration and Entrainment. <i>Curr Biol</i> 30, 2225-2237 e2225 (2020). T. Yoshi, T. Todo, C.			
 output in the Drosophila brain. <i>Eur J Neurosci</i> 51, 268-281 (220). X. Liang <i>et al.</i>, Morning and Evening Circadian Pacemakers Independently Drive Premotor Centers via a Specific Dopamine Relay. <i>Neuron</i> 102, 843-857 e844 (2019). F. Guo, M. Holla, M. M. Diaz, M. Rosbash, A Circadian Output Circuit Controls Sleep- Wake Arousal in Drosophila. <i>Neuron</i> 100, 624-635 e624 (2018). A. Lamaze, P. Kratschmer, K. F. Chen, S. Lowe, J. E. C. Jepson, A Wake-Promoting Circadian Output Circuit in Drosophila. <i>Curr Biol</i> 28, 3098-3105 e3093 (2018). C. Helfrich-Forster <i>et al.</i>, The lateral and dorsal neurons of Drosophila melanogaster: new insights about their morphology and function. <i>Cold Spring Harb Symp Quant Biol</i> 72, 517-525 (2007). A. Ramakrishnan, V. Sheeba, Gap junction protein Innexin2 modulates the period of free-running rhythms in Drosophila melanogaster. <i>IScience</i> 24, 103011 (2021). M. P. Fernandez, J. Berni, M. F. Ceriani, Circadian remodeling of neuronal circuits involved in rhythmic behavior. <i>PLoS Biol</i> 6, e69 (2008). J. M. Duhart <i>et al.</i>, Circadian Structural Plasticity Drives Remodeling of E Cell Output. <i>Curr Biol</i> 30, 5040-5048 e5045 (2020). B. J. Song, S. J. Sharp, D. Rogulja, Daily rewiring of a neural circuit generates a predictive model of environmental light. <i>Sci Adv</i> 7 (2021). X. Liang, T. E. Holy, P. H. Taghert, A Series of Suppressive Signals within the Drosophila Circadian Neural Circuit Generates Sequential Daily Outputs. <i>Neuron</i> 94, 1173-1189 e1174 (2017). F. Guo <i>et al.</i>, Circadian neuron feedback controls the Drosophila sleepactivity profile. <i>Nature</i> 556, 292-297 (2016). M. P. Fernandez <i>et al.</i>, Sites of Circadian Clock Neuron Plasticity Mediate Sensory Integration and Entrainment. <i>Curr Biol</i> 30, 2225-2237 e2225 (2020). T. Yoshii, T. Todo, C. Wulbeck, R. Stanewsky, C. Helfrich-Forster, Cryptochrome is present in the compound eyes and a subset of Drosophila's clock neur			
 X. Liang <i>et al.</i>, Morning and Evening Circadian Pacemakers Independently Drive Premotor Centers via a Specific Dopamine Relay. <i>Neuron</i> 102, 843-857 e844 (2019). F. Guo, M. Holla, M. M. Diaz, M. Rosbash, A. Circadian Output Circuit Controls Sleep- Wake Arousal in Drosophila. <i>Neuron</i> 100, 624-635 e624 (2018). A. Lamaze, P. Kratschmer, K. F. Chen, S. Lowe, J. E. C. Jepson, A Wake-Promoting Circadian Output Circuit in Drosophila. <i>Curr Biol</i> 28, 3098-3105 e3093 (2018). C. Helfrich-Forster <i>et al.</i>, The lateral and dorsal neurons of Drosophila melanogaster: new insights about their morphology and function. <i>Cold Spring Harb Symp Quant Biol</i> 72, 517-525 (2007). A. Ramakrishnan, V. Sheeba, Gap junction protein Innexin2 modulates the period of free-running rhythms in Drosophila melanogaster. <i>IScience</i> 24, 103011 (2021). M. P. Fernandez, J. Berni, M. F. Ceriani, Circadian remodeling of neuronal circuits involved in rhythmic behavior. <i>PLoS Biol</i> 6, e69 (2008). J. M. Duhart <i>et al.</i>, Circadian Structural Plasticity Drives Remodeling of E Cell Output. <i>Curr Biol</i> 30, 5040-5048 e5045 (2020). B. J. Song, S. J. Sharp, D. Rogulja, Daily rewiring of a neural circuit generates a predictive model of environmental light. <i>Sci Adv</i> 7 (2021). X. Liang, T. E. Holy, P. H. Taghert, A Series of Suppressive Signals within the Drosophila Circadian Neural Circuit Generates Sequential Daily Outputs. <i>Neuron</i> 94, 1173-1189 e1174 (2017). F. Guo <i>et al.</i>, Circadian neuron feedback controls the Drosophila sleepactivity profile. <i>Nature</i> 536, 292-297 (2016). M. P. Fernandez <i>et al.</i>, Sites of Circadian Clock Neuron Plasticity Mediate Sensory Integration and Entrainment. <i>Curr Biol</i> 30, 2225-2237 e2225 (2020). T. Yoshii, T. Todo, C. Wulbeck, R. Stanewsky, C. Helfrich-Forster, Cryptochrome is present in the compooud eyes and a subset of Drosophila's clock neurons. <i></i>		44.	
 Premotor Centers via a Specific Dopamine Relay. Neuron 102, 843-857 e844 (2019). F. Guo, M. Holla, M. M. Diaz, M. Rosbash, A Circadian Output Circuit Controls Steep-Wake Arousal in Drosophila. Neuron 100, 624-635 e624 (2018). A. Lamaze, P. Kratschmer, K. F. Chen, S. Lowe, J. E. C. Jepson, A Wake-Promoting Circadian Output Circuit in Drosophila. Curr Biol 28, 3098-3105 e3093 (2018). C. Helfrich-Forster <i>et al.</i>, The lateral and dorsal neurons of Drosophila melanogaster: new insights about their morphology and function. Cold Spring Harb Symp Quant Biol 72, 517-525 (2007). A. Ramakrishnan, V. Sheeba, Gap junction protein Innexin2 modulates the period of free-running rhythms in Drosophila melanogaster. <i>iScience</i> 24, 103011 (2021). M. P. Fernandez, J. Berni, M. F. Ceriani, Circadian remodeling of neuronal circuits involved in rhythmic behavior. PLoS Biol 6, e69 (2008). J. M. Duhart <i>et al.</i>, Circadian Structural Plasticity Drives Remodeling of E Cell Output. <i>Curr Biol</i> 30, 5040-5048 e5045 (2020). B. J. Song, S. J. Sharp, D. Rogulja, Daily rewiring of a neural circuit generates a predictive model of environmental light. <i>Sci Adv</i> 7 (2021). X. Liang, T. E. Holy, P. H. Taghert, A Series of Suppressive Signals within the Drosophila Circadian Neural Circuit Generates Sequential Daily Outputs. <i>Neuron</i> 94, 1173-1189 e1174 (2017). F. Guo <i>et al.</i>, Circadian neuron feedback controls the Drosophila Seepactivity profile. <i>Nature</i> 556, 292-297 (2016). S. Yadlapalli <i>et al.</i>, Sites of Circadian Clock Neuron Plasticity Mediate Sensory Integration and Entrainment. <i>Curr Biol</i> 30, 2225-2237 e2225 (2020). T. Yoshii, T. Todo, C. Wulbeck, R. Stanewsky, C. Helfrich-Forster, Cryptochrome is present in the compound eyes and a subset of Drosophila's clock neurons. <i>J Comp Neurol</i> 508, 952-966 (2008). T. Yoshii, C. Hermann, C. Helfrich-Forster, Cryptochrome-positive an			
 F. Guo, M. Holla, M. M. Diaz, M. Rosbash, A Circadian Output Circuit Controls Sleep- Wake Arousal in Drosophila. <i>Neuron</i> 100, 624-635 e624 (2018). A. Lamaze, P. Kratschmer, K. F. Chen, S. Lowe, J. E. C. Jepson, A Wake-Promoting Circadian Output Circuit in Drosophila. <i>Curr Biol</i> 28, 3098-3105 e3093 (2018). C. Helfrich-Forster <i>et al.</i>, The lateral and dorsal neurons of Drosophila melanogaster: new insights about their morphology and function. <i>Cold Spring Harb Symp Quant Biol</i> 72, 517-525 (2007). A. Ramakrishnan, V. Sheeba, Gap junction protein Innexin2 modulates the period of free-running rhythms in Drosophila melanogaster. <i>iScience</i> 24, 103011 (2021). M. P. Fernandez, J. Berni, M. F. Ceriani, Circadian remodeling of neuronal circuits involved in rhythmic behavior. <i>PLoS Biol</i> 6, e69 (2008). J. M. Duhart <i>et al.</i>, Circadian Structural Plasticity Drives Remodeling of E Cell Output. <i>Curr Biol</i> 30, 5040-5048 e5045 (2020). B. J. Song, S. J. Sharp, D. Rogulja, Daily rewiring of a neural circuit generates a predictive model of environmental light. <i>Sci Adv</i> 7 (2021). X. Liang, T. E. Holy, P. H. Taghert, A Series of Suppressive Signals within the Drosophila Circadian neuron feedback controls the Drosophila sleepactivity profile. <i>Nature</i> 536, 292-297 (2016). S. Yadlapalli <i>et al.</i>, Circadian clock neurons constantly monitor environmental temperature to set sleep timing. <i>Nature</i> 555, 98-102 (2018). M. P. Fernandez <i>et al.</i>, Sites of Circadian Clock Neuron Plasticity Mediate Sensory Integration and Entrainment. <i>Curr Biol</i> 30, 2225-2237 e225 (2020). T. Yoshii, T. Todo, C. Wulbeck, R. Stanewsky, C. Helfrich-Forster, Cryptochrome is present in the compound eyes and a subset of Drosophila's clock neurons. <i>J Comp Neurol</i> 508, 952-966 (2008). E. Marder, D. Bucher, D. J. Schulz, A. L. Taylor, Invertebrate central pattern generation moves along.		45.	
 Wake Arousal in Drosophila. Neuron 100, 624-635 e624 (2018). A. Lamaze, P. Kratschmer, K. F. Chen, S. Lowe, J. E. C. Jepson, A Wake-Promoting Circadian Output Circuit in Drosophila. Curr Biol 28, 3098-3105 e3093 (2018). C. Helfrich-Forster <i>et al.</i>, The lateral and dorsal neurons of Drosophila melanogaster: new insights about their morphology and function. Cold Spring Harb Symp Quant Biol 72, 517-525 (2007). A. Ramakrishnan, V. Sheeba, Gap junction protein Innexin2 modulates the period of free-running rhythms in Drosophila melanogaster. <i>IScience</i> 24, 103011 (2021). M. P. Fernandez, J. Berni, M. F. Ceriani, Circadian remodeling of neuronal circuits involved in rhythmic behavior. <i>PLoS Biol</i> 6, e69 (2008). J. M. Duhart <i>et al.</i>, Circadian Structural Plasticity Drives Remodeling of E Cell Output. <i>Curr Biol</i> 30, 5040-5048 e5045 (2020). B. J. Song, S. J. Sharp, D. Rogulja, Daily rewiring of a neural circuit generates a predictive model of environmental light. <i>Sci Adv</i> 7 (2021). X. Liang, T. E. Holy, P. H. Taghert, A Series of Suppressive Signals within the Drosophila Circadian Neural Circuit Generates Sequential Daily Outputs. <i>Neuron</i> 94, 1173-1189 e1174 (2017). F. Guo <i>et al.</i>, Circadian neuron feedback controls the Drosophila sleepactivity profile. <i>Nature</i> 536, 292-297 (2016). S. Yadlapalli <i>et al.</i>, Circadian clock neurons constantly monitor environmental temperature to set sleep timing. <i>Nature</i> 555, 98-102 (2018). M. P. Fernandez <i>et al.</i>, Sites of Circadian Clock Neuron Plasticity Mediate Sensory Integration and Entrainment. <i>Curr Biol</i> 30, 2225-2237 e2225 (2020). T. Yoshii, T. Todo, C. Wulbeck, R. Stanewsky, C. Helfrich-Forster, Cryptochrome is present in the compound eyes and a subset of Drosophila's clock neurons. <i>J Comp Neurol</i> 508, 952-966 (2008). S. T. Yoshii, C. Hermann, C. Helfrich-Forster, Cryptochrome-positive and -negative clock neurons in Drosophila entrain differentially to			
 A. Lamaze, P. Kratschmer, K. F. Chen, S. Lowe, J. E. C. Jepson, A Wake-Promoting Circadian Output Circuit in Drosophila. <i>Curr Biol</i> 28, 3098-3105 e3093 (2018). C. Helfrich-Forster <i>et al.</i>, The lateral and dorsal neurons of Drosophila melanogaster: new insights about their morphology and function. <i>Cold Spring Harb Symp Quant Biol</i> 72, 517-525 (2007). A. Ramakrishnan, V. Sheeba, Gap junction protein Innexin2 modulates the period of free-running rhythms in Drosophila melanogaster. <i>IScience</i> 24, 103011 (2021). M. P. Fernandez, J. Berni, M. F. Ceriani, Circadian remodeling of neuronal circuits involved in rhythmic behavior. <i>PLoS Biol</i> 6, e69 (2008). J. M. Duhart <i>et al.</i>, Circadian Structural Plasticity Drives Remodeling of E Cell Output. <i>Curr Biol</i> 30, 5040-5048 e5045 (2020). B. J. Song, S. J. Sharp, D. Rogulja, Daily rewiring of a neural circuit generates a predictive model of environmental light. <i>Sci Adv</i> 7 (2021). X. Liang, T. E. Holy, P. H. Taghert, A Series of Suppressive Signals within the Drosophila Circadian neuron feedback controls the Drosophila sleepactivity profile. <i>Nature</i> 356, 292-297 (2016). F. Guo <i>et al.</i>, Circadian neuron feedback controls the Drosophila sleepactivity profile. <i>Nature</i> 356, 292-297 (2016). M. P. Fernandez <i>et al.</i>, Sites of Circadian Clock Neuron Plasticity Mediate Sensory Integration and Entrainment. <i>Curr Biol</i> 30, 2225-2237 e2225 (2020). T. Yoshii, T. Todo, C. Wulbeck, R. Stanewsky, C. Helfrich-Forster, Cryptochrome is present in the compound eyes and a subset of Drosophila's clock neurons. <i>J Comp Neurol</i> 508, 952-966 (2008). T. Yoshii, C. Hermann, C. Helfrich-Forster, Cryptochrome-positive and -negative clock neurons in Drosophila entrain differentially to light and temperature. <i>J Biol Rhythms</i> 25, 387-398 (2010). E. Marder, D. Bucher, D. J. Schulz, A. L. Taylor, Invertebrate central pattern generation moves a		46.	
 Circadian Output Circuit in Drosophila. <i>Curr Biol</i> 28, 3098-3105 e3093 (2018). C. Helfrich-Forster <i>et al.</i>, The lateral and dorsal neurons of Drosophila melanogaster: new insights about their morphology and function. <i>Cold Spring Harb Symp Quant Biol</i> 72, 517-525 (2007). A. Ramakrishnan, V. Sheeba, Gap junction protein Innexin2 modulates the period of free-running rhythms in Drosophila melanogaster. <i>Iscience</i> 24, 103011 (2021). M. P. Fernandez, J. Berni, M. F. Ceriani, Circadian remodeling of neuronal circuits involved in rhythmic behavior. <i>PLoS Biol</i> 6, e69 (2008). J. M. Duhart <i>et al.</i>, Circadian Structural Plasticity Drives Remodeling of E Cell Output. <i>Curr Biol</i> 30, 5040-5048 e5045 (2020). B. J. Song, S. J. Sharp, D. Rogulja, Daily rewring of a neural circuit generates a predictive model of environmental light. <i>Sci Adv</i> 7 (2021). X. Liang, T. E. Holy, P. H. Taghert, A Series of Suppressive Signals within the Drosophila Circadian Neural Circuit Generates Sequential Daily Outputs. <i>Neuron</i> 94, 1173-1189 e1174 (2017). F. Guo <i>et al.</i>, Circadian neuron feedback controls the Drosophila sleepactivity profile. <i>Nature</i> 536, 292-297 (2016). S. Yadlapalli <i>et al.</i>, Circadian clock neurons constantly monitor environmental temperature to set sleep timing. <i>Nature</i> 555, 98-102 (2018). M. P. Fernandez <i>et al.</i>, Sites of Circadian Clock Neuron Plasticity Mediate Sensory Integration and Entrainment. <i>Curr Biol</i> 30, 2225-2237 e2225 (2020). T. Yoshii, T. Todo, C. Wulbeck, R. Stanewsky, C. Helfrich-Forster, Cryptochrome is present in the compound eyes and a subset of Drosophila's clock neurons. <i>J Comp Neurol</i> 508, 952-966 (2008). S. Marder, D. Bucher, D. J. Schulz, A. L. Taylor, Invertebrate central pattern generation moves along. <i>Curr Biol</i> 31, R685-699 (2005). A. I. Selverston, J. P. Miller, Mechanisms underlying pattern generation in lobster stom			
 48. C. Helfrich-Forster <i>et al.</i>, The lateral and dorsal neurons of Drosophila melanogaster: new insights about their morphology and function. <i>Cold Spring Harb Symp Quant Biol</i> 72, 517-525 (2007). 49. A. Ramakrishnan, V. Sheeba, Gap junction protein Innexin2 modulates the period of free-running rhythms in Drosophila melanogaster. <i>iScience</i> 24, 103011 (2021). 50. M. P. Fernandez, J. Berni, M. F. Ceriani, Circadian remodeling of neuronal circuits involved in rhythmic behavior. <i>PLoS Biol</i> 6, e69 (2008). 51. J. M. Duhart <i>et al.</i>, Circadian Structural Plasticity Drives Remodeling of E Cell Output. <i>Curr Biol</i> 30, 5040-5048 e5045 (2020). 52. B. J. Song, S. J. Sharp, D. Rogulja, Daily rewiring of a neural circuit generates a predictive model of environmental light. <i>Sci Adv</i> 7 (2021). 53. X. Liang, T. E. Holy, P. H. Taghert, A Series of Suppressive Signals within the Drosophila Circadian Neural Circuit Generates Sequential Daily Outputs. <i>Neuron</i> 94, 1173-1189 e1174 (2017). 54. F. Guo <i>et al.</i>, Circadian neuron feedback controls the Drosophila sleepactivity profile. <i>Nature</i> 536, 292-297 (2016). 55. S. Yadlapalli <i>et al.</i>, Circadian clock neurons constantly monitor environmental temperature to set sleep timing. <i>Nature</i> 555, 98-102 (2018). 57. T. Yoshii, T. Todo, C. Wulbeck, R. Stanewsky, C. Helfrich-Forster, Cryptochrome is present in the compound eyes and a subset of Drosophila's clock neurons. <i>J Comp Neurol</i> 508, 952-966 (2008). 58. T. Yoshii, C. Hermann, C. Helfrich-Forster, Cryptochrome-positive and -negative clock neurons in Drosophila entrain differentially to light and temperature. <i>J Biol Rhythms</i> 25, 387-398 (2010). 59. E. Marder, D. Bucher, D. J. Schulz, A. L. Taylor, Invertebrate central pattern generation moves along. <i>Curr Biol</i> 15, R685-699 (2005). 60. A. I. Selverston, J. P. Miller, Mechanisms underlying pattern generati		47.	
 new insights about their morphology and function. <i>Cold Spring Harb Symp Quant Biol</i> 72, 517-525 (2007). 49. A. Ramakrishnan, V. Sheeba, Gap junction protein Innexin2 modulates the period of free-running rhythms in Drosophila melanogaster. <i>iScience</i> 24, 103011 (2021). 50. M. P. Fernandez, J. Berni, M. F. Ceriani, Circadian remodeling of neuronal circuits involved in rhythmic behavior. <i>PLoS Biol</i> 6, e69 (2008). 51. J. M. Duhart <i>et al.</i>, Circadian Structural Plasticity Drives Remodeling of E Cell Output. <i>Curr Biol</i> 30, 5040-5048 e5045 (2020). 52. B. J. Song, S. J. Sharp, D. Rogulja, Daily rewiring of a neural circuit generates a predictive model of environmental light. <i>Sci Adv</i> 7 (2021). 53. X. Liang, T. E. Holy, P. H. Taghert, A Series of Suppressive Signals within the Drosophila Circadian Neural Circuit Generates Sequential Daily Outputs. <i>Neuron</i> 94, 1173-1189 e1174 (2017). 54. F. Guo <i>et al.</i>, Circadian neuron feedback controls the Drosophila sleepactivity profile. <i>Nature</i> 536, 292-297 (2016). 55. S. Yadlapalli <i>et al.</i>, Circadian clock neurons constantly monitor environmental temperature to set sleep timing. <i>Nature</i> 555, 98-102 (2018). 55. M. P. Fernandez <i>et al.</i>, Sites of Circadian Clock Neuron Plasticity Mediate Sensory Integration and Entrainment. <i>Curr Biol</i> 30, 2225-2237 e2225 (2020). 57. T. Yoshii, T. Todo, C. Wulbeck, R. Stanewsky, C. Helfrich-Forster, Cryptochrome is present in the compound eyes and a subset of Drosophila's clock neurons. <i>J Comp Neurol</i> 58, 952-966 (2008). 58. T. Yoshii, C. Hermann, C. Helfrich-Forster, Cryptochrome-positive and -negative clock neurons in Drosophila entrain differentially to light and temperature. <i>J Biol Rhythms</i> 25, 387-398 (2010). 59. E. Marder, D. Bucher, D. J. Schulz, A. L. Taylor, Invertebrate central pattern generation moves along. <i>Curr Biol</i> 15, R685-699 (2005). 59. E. Marder, D. Bucher, D. J. Schulz, A. L. T			
 72, 517-525 (2007). A. Ramakrishnan, V. Sheeba, Gap junction protein Innexin2 modulates the period of free-running rhythms in Drosophila melanogaster. <i>iScience</i> 24, 103011 (2021). M. P. Fernandez, J. Berni, M. F. Ceriani, Circadian remodeling of neuronal circuits involved in rhythmic behavior. <i>PLoS Biol</i> 6, e69 (2008). J. M. Duhart <i>et al.</i>, Circadian Structural Plasticity Drives Remodeling of E Cell Output. <i>Curr Biol</i> 30, 5040-5048 e5045 (2020). B. J. Song, S. J. Sharp, D. Rogulja, Daily rewiring of a neural circuit generates a predictive model of environmental light. <i>Sci Adv</i> 7 (2021). X. Liang, T. E. Holy, P. H. Taghert, A Series of Suppressive Signals within the Drosophila Circadian Neural Circuit Generates Sequential Daily Outputs. <i>Neuron</i> 94, 1173-1189 e1174 (2017). F. Guo <i>et al.</i>, Circadian neuron feedback controls the Drosophila sleepactivity profile. <i>Nature</i> 536, 292-297 (2016). S. Yadlapalli <i>et al.</i>, Circadian clock neurons constantly monitor environmental temperature to set sleep timing. <i>Nature</i> 555, 98-102 (2018). M. P. Fernandez <i>et al.</i>, Sites of Circadian Clock Neuron Plasticity Mediate Sensory Integration and Entrainment. <i>Curr Biol</i> 30, 2225-2237 e2225 (2020). T. Yoshii, T. Todo, C. Wulbeck, R. Stanewsky, C. Helfrich-Forster, Cryptochrome is present in the compound eyes and a subset of Drosophila's clock neurons. <i>J Comp Neurol</i> 508, 952-966 (2008). T. Yoshii, C. Hermann, C. Helfrich-Forster, Cryptochrome-positive and -negative clock neurons in Drosophila entrain differentially to light and temperature. <i>J Biol Rhythms</i> 25, 387-398 (2010). E. Marder, D. Bucher, D. J. Schulz, A. L. Taylor, Invertebrate central pattern generation moves along. <i>Curr Biol</i> 35, Re85-699 (2005). A. I. Selverston, J. P. Miller, Mechanisms underlying pattern generation in lobster stomatogastric ganglion as determined by selective inactivation of identified neurons. I. 		48.	
 49. A. Ramakrishnan, V. Sheeba, Gap junction protein Innexin2 modulates the period of free-running rhythms in Drosophila melanogaster. <i>IScience</i> 24, 103011 (2021). 1035 50. M. P. Fernandez, J. Berni, M. F. Ceriani, Circadian remodeling of neuronal circuits involved in rhythmic behavior. <i>PLoS Biol</i> 6, e69 (2008). 1037 51. J. M. Duhart <i>et al.</i>, Circadian Structural Plasticity Drives Remodeling of E Cell Output. <i>Curr Biol</i> 30, 5040-5048 e5045 (2020). 1038 52. B. J. Song, S. J. Sharp, D. Rogulja, Daily rewiring of a neural circuit generates a predictive model of environmental light. <i>Sci Adv</i> 7 (2021). 1041 53. X. Liang, T. E. Holy, P. H. Taghert, A Series of Suppressive Signals within the Drosophila Circadian Neural Circuit Generates Sequential Daily Outputs. <i>Neuron</i> 94, 1173-1189 e1174 (2017). 1044 54. F. Guo <i>et al.</i>, Circadian neuron feedback controls the Drosophila sleepactivity profile. <i>Nature</i> 536, 292-297 (2016). 1046 55. S. Yadlapalli <i>et al.</i>, Circadian clock neurons constantly monitor environmental temperature to set sleep timing. <i>Nature</i> 555, 98-102 (2018). 1048 56. M. P. Fernandez <i>et al.</i>, Sites of Circadian Clock Neuron Plasticity Mediate Sensory Integration and Entrainment. <i>Curr Biol</i> 30, 2225-2237 e2225 (2020). 1050 57. T. Yoshii, T. Todo, C. Wulbeck, R. Stanewsky, C. Helfrich-Forster, Cryptochrome is present in the compound eyes and a subset of Drosophila's clock neurons. <i>J Comp Neurol</i> 508, 952-966 (2008). 1053 58. T. Yoshii, C. Hermann, C. Helfrich-Forster, Cryptochrome-positive and -negative clock neurons in Drosophila entrain differentially to light and temperature. <i>J Biol Rhythms</i> 25, 387-398 (2010). 1056 59. E. Marder, D. Bucher, D. J. Schulz, A. L. Taylor, Invertebrate central pattern generation moves along. <i>Curr Biol</i> 15, R685-699 (2005). 1051 60. A. I. Selverston, J. P. Miller, Mechanisms underlying pattern generation in l			
 free-running rhythms in Drosophila melanogaster. <i>iScience</i> 24, 103011 (2021). M. P. Fernandez, J. Berni, M. F. Ceriani, Circadian remodeling of neuronal circuits involved in rhythmic behavior. <i>PLoS Biol</i> 6, e69 (2008). J. M. Duhart <i>et al.</i>, Circadian Structural Plasticity Drives Remodeling of E Cell Output. <i>Curr Biol</i> 30, 5040-5048 e5045 (2020). B. J. Song, S. J. Sharp, D. Rogulja, Daily rewiring of a neural circuit generates a predictive model of environmental light. <i>Sci Adv</i> 7 (2021). X. Liang, T. E. Holy, P. H. Taghert, A Series of Suppressive Signals within the Drosophila Circadian Neural Circuit Generates Sequential Daily Outputs. <i>Neuron</i> 94, 1173-1189 e1174 (2017). F. Guo <i>et al.</i>, Circadian neuron feedback controls the Drosophila sleepactivity profile. <i>Nature</i> 536, 292-297 (2016). S. Yadlapalli <i>et al.</i>, Circadian clock neurons constantly monitor environmental temperature to set sleep timing. <i>Nature</i> 555, 98-102 (2018). M. P. Fernandez <i>et al.</i>, Sites of Circadian Clock Neuron Plasticity Mediate Sensory Integration and Entrainment. <i>Curr Biol</i> 30, 2225-2237 e2225 (2020). T. Yoshii, T. Todo, C. Wulbeck, R. Stanewsky, C. Helfrich-Forster, Cryptochrome is present in the compound eyes and a subset of Drosophila's clock neurons. <i>J Comp</i> <i>Neurol</i> 508, 952-966 (2008). T. Yoshii, C. Hermann, C. Helfrich-Forster, Cryptochrome-positive and -negative clock neurons in Drosophila entrain differentially to light and temperature. <i>J Biol Rhythms</i> 25, 387-398 (2010). E. Marder, D. Bucher, D. J. Schulz, A. L. Taylor, Invertebrate central pattern generation moves along. <i>Curr Biol</i> 15, R685-699 (2005). A. I. Selverston, J. P. Miller, Mechanisms underlying pattern generation in lobster stomatogastric ganglion as determined by selective inactivation of identified neurons. I. 			
 M. P. Fernandez, J. Berni, M. F. Ceriani, Circadian remodeling of neuronal circuits involved in rhythmic behavior. <i>PLoS Biol</i> 6, e69 (2008). J. M. Duhart <i>et al.</i>, Circadian Structural Plasticity Drives Remodeling of E Cell Output. <i>Curr Biol</i> 30, 5040-5048 e5045 (2020). B. J. Song, S. J. Sharp, D. Rogulja, Daily rewiring of a neural circuit generates a predictive model of environmental light. <i>Sci Adv</i> 7 (2021). X. Liang, T. E. Holy, P. H. Taghert, A Series of Suppressive Signals within the Drosophila Circadian Neural Circuit Generates Sequential Daily Outputs. <i>Neuron</i> 94, 1173-1189 e1174 (2017). F. Guo <i>et al.</i>, Circadian neuron feedback controls the Drosophila sleepactivity profile. <i>Nature</i> 536, 292-297 (2016). S. Yadlapalli <i>et al.</i>, Circadian clock neurons constantly monitor environmental temperature to set sleep timing. <i>Nature</i> 555, 98-102 (2018). M. P. Fernandez <i>et al.</i>, Sites of Circadian Clock Neuron Plasticity Mediate Sensory Integration and Entrainment. <i>Curr Biol</i> 30, 2225-2237 e2225 (2020). T. Yoshii, T. Todo, C. Wulbeck, R. Stanewsky, C. Helfrich-Forster, Cryptochrome is present in the compound eyes and a subset of Drosophila's clock neurons. <i>J Comp</i> <i>Neurol</i> 508, 952-966 (2008). T. Yoshii, C. Hermann, C. Helfrich-Forster, Cryptochrome-positive and -negative clock neurons in Drosophila entrain differentially to light and temperature. <i>J Biol Rhythms</i> 25, 387-398 (2010). E. Marder, D. Bucher, D. J. Schulz, A. L. Taylor, Invertebrate central pattern generation moves along. <i>Curr Biol</i> 15, R685-699 (2005). A. I. Selverston, J. P. Miller, Mechanisms underlying pattern generation in lobster stomatogastric ganglion as determined by selective inactivation of identified neurons. I. 		49.	
 involved in rhythmic behavior. <i>PLoS Biol</i> 6, e69 (2008). J. M. Duhart <i>et al.</i>, Circadian Structural Plasticity Drives Remodeling of E Cell Output. <i>Curr Biol</i> 30, 5040-5048 e5045 (2020). B. J. Song, S. J. Sharp, D. Rogulja, Daily rewiring of a neural circuit generates a predictive model of environmental light. <i>Sci Adv</i> 7 (2021). X. Liang, T. E. Holy, P. H. Taghert, A Series of Suppressive Signals within the Drosophila Circadian Neural Circuit Generates Sequential Daily Outputs. <i>Neuron</i> 94, 1173-1189 e1174 (2017). F. Guo <i>et al.</i>, Circadian neuron feedback controls the Drosophila sleepactivity profile. <i>Nature</i> 536, 292-297 (2016). S. Yadlapalli <i>et al.</i>, Circadian clock neurons constantly monitor environmental temperature to set sleep timing. <i>Nature</i> 555, 98-102 (2018). M. P. Fernandez <i>et al.</i>, Sites of Circadian Clock Neuron Plasticity Mediate Sensory Integration and Entrainment. <i>Curr Biol</i> 30, 2225-2237 e2225 (2020). T. Yoshii, T. Todo, C. Wulbeck, R. Stanewsky, C. Helfrich-Forster, Cryptochrome is present in the compound eyes and a subset of Drosophila's clock neurons. <i>J Comp</i> <i>Neurol</i> 508, 952-966 (2008). S. T. Yoshii, C. Hermann, C. Helfrich-Forster, Cryptochrome-positive and -negative clock neurons in Drosophila entrain differentially to light and temperature. <i>J Biol Rhythms</i> 25, 387-398 (2010). E. Marder, D. Bucher, D. J. Schulz, A. L. Taylor, Invertebrate central pattern generation moves along. <i>Curr Biol</i> 15, R685-699 (2005). A. I. Selverston, J. P. Miller, Mechanisms underlying pattern generation in lobster stomatogastric ganglion as determined by selective inactivation of identified neurons. I. 			
 J. M. Duhart <i>et al.</i>, Circadian Structural Plasticity Drive's Remodeling of E Cell Output. <i>Curr Biol</i> 30, 5040-5048 e5045 (2020). B. J. Song, S. J. Sharp, D. Rogulja, Daily rewiring of a neural circuit generates a predictive model of environmental light. <i>Sci Adv</i> 7 (2021). X. Liang, T. E. Holy, P. H. Taghert, A Series of Suppressive Signals within the Drosophila Circadian Neural Circuit Generates Sequential Daily Outputs. <i>Neuron</i> 94, 1173-1189 e1174 (2017). F. Guo <i>et al.</i>, Circadian neuron feedback controls the Drosophila sleepactivity profile. <i>Nature</i> 536, 292-297 (2016). S. Yadlapalli <i>et al.</i>, Circadian clock neurons constantly monitor environmental temperature to set sleep timing. <i>Nature</i> 555, 98-102 (2018). M. P. Fernandez <i>et al.</i>, Sites of Circadian Clock Neuron Plasticity Mediate Sensory Integration and Entrainment. <i>Curr Biol</i> 30, 2225-2237 e2225 (2020). T. Yoshii, T. Todo, C. Wulbeck, R. Stanewsky, C. Helfrich-Forster, Cryptochrome is present in the compound eyes and a subset of Drosophila's clock neurons. <i>J Comp</i> <i>Neurol</i> 508, 952-966 (2008). T. Yoshii, C. Hermann, C. Helfrich-Forster, Cryptochrome-positive and -negative clock neurons in Drosophila entrain differentially to light and temperature. <i>J Biol Rhythms</i> 25, 387-398 (2010). E. Marder, D. Bucher, D. J. Schulz, A. L. Taylor, Invertebrate central pattern generation moves along. <i>Curr Biol</i> 15, R685-699 (2005). A. I. Selverston, J. P. Miller, Mechanisms underlying pattern generation in lobster stomatogastric ganglion as determined by selective inactivation of identified neurons. I. 		50.	
 Curr Biol 30, 5040-5048 e5045 (2020). B. J. Song, S. J. Sharp, D. Rogulja, Daily rewiring of a neural circuit generates a predictive model of environmental light. <i>Sci Adv</i> 7 (2021). X. Liang, T. E. Holy, P. H. Taghert, A Series of Suppressive Signals within the Drosophila Circadian Neural Circuit Generates Sequential Daily Outputs. <i>Neuron</i> 94, 1173-1189 e1174 (2017). F. Guo <i>et al.</i>, Circadian neuron feedback controls the Drosophila sleepactivity profile. <i>Nature</i> 536, 292-297 (2016). S. Yadlapalli <i>et al.</i>, Circadian clock neurons constantly monitor environmental temperature to set sleep timing. <i>Nature</i> 555, 98-102 (2018). M. P. Fernandez <i>et al.</i>, Sites of Circadian Clock Neuron Plasticity Mediate Sensory Integration and Entrainment. <i>Curr Biol</i> 30, 2225-2237 e2225 (2020). T. Yoshii, T. Todo, C. Wulbeck, R. Stanewsky, C. Helfrich-Forster, Cryptochrome is present in the compound eyes and a subset of Drosophila's clock neurons. <i>J Comp Neurol</i> 508, 952-966 (2008). T. Yoshii, C. Hermann, C. Helfrich-Forster, Cryptochrome-positive and -negative clock neurons in Drosophila entrain differentially to light and temperature. <i>J Biol Rhythms</i> 25, 387-398 (2010). E. Marder, D. Bucher, D. J. Schulz, A. L. Taylor, Invertebrate central pattern generation moves along. <i>Curr Biol</i> 15, R685-699 (2005). A. I. Selverston, J. P. Miller, Mechanisms underlying pattern generation in lobster stomatogastric ganglion as determined by selective inactivation of identified neurons. I. 			
 52. B. J. Song, S. J. Sharp, D. Rogulja, Daily rewiring of a neural circuit generates a predictive model of environmental light. <i>Sci Adv</i> 7 (2021). 53. X. Liang, T. E. Holy, P. H. Taghert, A Series of Suppressive Signals within the Drosophila Circadian Neural Circuit Generates Sequential Daily Outputs. <i>Neuron</i> 94, 1173-1189 e1174 (2017). 54. F. Guo <i>et al.</i>, Circadian neuron feedback controls the Drosophila sleepactivity profile. <i>Nature</i> 536, 292-297 (2016). 55. S. Yadlapalli <i>et al.</i>, Circadian clock neurons constantly monitor environmental temperature to set sleep timing. <i>Nature</i> 555, 98-102 (2018). 56. M. P. Fernandez <i>et al.</i>, Sites of Circadian Clock Neuron Plasticity Mediate Sensory Integration and Entrainment. <i>Curr Biol</i> 30, 2225-2237 e2225 (2020). 57. T. Yoshii, T. Todo, C. Wulbeck, R. Stanewsky, C. Helfrich-Forster, Cryptochrome is present in the compound eyes and a subset of Drosophila's clock neurons. <i>J Comp Neurol</i> 508, 952-966 (2008). 58. T. Yoshii, C. Hermann, C. Helfrich-Forster, Cryptochrome-positive and -negative clock neurons in Drosophila entrain differentially to light and temperature. <i>J Biol Rhythms</i> 25, 387-398 (2010). 59. E. Marder, D. Bucher, D. J. Schulz, A. L. Taylor, Invertebrate central pattern generation moves along. <i>Curr Biol</i> 15, R685-699 (2005). 60. A. I. Selverston, J. P. Miller, Mechanisms underlying pattern generation in lobster stomatogastric ganglion as determined by selective inactivation of identified neurons. I. 		51.	
 predictive model of environmental light. <i>Sci Adv</i> 7 (2021). X. Liang, T. E. Holy, P. H. Taghert, A Series of Suppressive Signals within the Drosophila Circadian Neural Circuit Generates Sequential Daily Outputs. <i>Neuron</i> 94, 1173-1189 e1174 (2017). F. Guo <i>et al.</i>, Circadian neuron feedback controls the Drosophila sleepactivity profile. <i>Nature</i> 536, 292-297 (2016). S. Yadlapalli <i>et al.</i>, Circadian clock neurons constantly monitor environmental temperature to set sleep timing. <i>Nature</i> 555, 98-102 (2018). M. P. Fernandez <i>et al.</i>, Sites of Circadian Clock Neuron Plasticity Mediate Sensory Integration and Entrainment. <i>Curr Biol</i> 30, 2225-2237 e2225 (2020). T. Yoshii, T. Todo, C. Wulbeck, R. Stanewsky, C. Helfrich-Forster, Cryptochrome is present in the compound eyes and a subset of Drosophila's clock neurons. <i>J Comp</i> <i>Neurol</i> 508, 952-966 (2008). T. Yoshii, C. Hermann, C. Helfrich-Forster, Cryptochrome-positive and -negative clock neurons in Drosophila entrain differentially to light and temperature. <i>J Biol Rhythms</i> 25, 387-398 (2010). E. Marder, D. Bucher, D. J. Schulz, A. L. Taylor, Invertebrate central pattern generation moves along. <i>Curr Biol</i> 15, R685-699 (2005). A. I. Selverston, J. P. Miller, Mechanisms underlying pattern generation in lobster stomatogastric ganglion as determined by selective inactivation of identified neurons. I. 			
 1041 53. X. Liang, T. E. Holy, P. H. Taghert, A Series of Suppressive Signals within the Drosophila Circadian Neural Circuit Generates Sequential Daily Outputs. <i>Neuron</i> 94, 1173-1189 e1174 (2017). 1044 54. F. Guo <i>et al.</i>, Circadian neuron feedback controls the Drosophila sleepactivity profile. <i>Nature</i> 536, 292-297 (2016). 1046 55. S. Yadlapalli <i>et al.</i>, Circadian clock neurons constantly monitor environmental temperature to set sleep timing. <i>Nature</i> 555, 98-102 (2018). 1048 56. M. P. Fernandez <i>et al.</i>, Sites of Circadian Clock Neuron Plasticity Mediate Sensory Integration and Entrainment. <i>Curr Biol</i> 30, 2225-2237 e2225 (2020). 1050 57. T. Yoshii, T. Todo, C. Wulbeck, R. Stanewsky, C. Helfrich-Forster, Cryptochrome is present in the compound eyes and a subset of Drosophila's clock neurons. <i>J Comp</i> <i>Neurol</i> 508, 952-966 (2008). 1053 58. T. Yoshii, C. Hermann, C. Helfrich-Forster, Cryptochrome-positive and -negative clock neurons in Drosophila entrain differentially to light and temperature. <i>J Biol Rhythms</i> 25, 387-398 (2010). 1056 59. E. Marder, D. Bucher, D. J. Schulz, A. L. Taylor, Invertebrate central pattern generation moves along. <i>Curr Biol</i> 15, R685-699 (2005). 1058 60. A. I. Selverston, J. P. Miller, Mechanisms underlying pattern generation in lobster stomatogastric ganglion as determined by selective inactivation of identified neurons. I. 		52.	
 Drosophila Circadian Neural Circuit Generates Sequential Daily Outputs. <i>Neuron</i> 94, 1173-1189 e1174 (2017). F. Guo <i>et al.</i>, Circadian neuron feedback controls the Drosophila sleepactivity profile. <i>Nature</i> 536, 292-297 (2016). S. Yadlapalli <i>et al.</i>, Circadian clock neurons constantly monitor environmental temperature to set sleep timing. <i>Nature</i> 555, 98-102 (2018). M. P. Fernandez <i>et al.</i>, Sites of Circadian Clock Neuron Plasticity Mediate Sensory Integration and Entrainment. <i>Curr Biol</i> 30, 2225-2237 e2225 (2020). T. Yoshii, T. Todo, C. Wulbeck, R. Stanewsky, C. Helfrich-Forster, Cryptochrome is present in the compound eyes and a subset of Drosophila's clock neurons. <i>J Comp Neurol</i> 508, 952-966 (2008). T. Yoshii, C. Hermann, C. Helfrich-Forster, Cryptochrome-positive and -negative clock neurons in Drosophila entrain differentially to light and temperature. <i>J Biol Rhythms</i> 25, 387-398 (2010). E. Marder, D. Bucher, D. J. Schulz, A. L. Taylor, Invertebrate central pattern generation moves along. <i>Curr Biol</i> 15, R685-699 (2005). A. I. Selverston, J. P. Miller, Mechanisms underlying pattern generation in lobster stomatogastric ganglion as determined by selective inactivation of identified neurons. I. 			
 1043 1173-1189 e1174 (2017). 1044 54. F. Guo et al., Circadian neuron feedback controls the Drosophila sleepactivity profile. Nature 536, 292-297 (2016). 1046 55. S. Yadlapalli et al., Circadian clock neurons constantly monitor environmental temperature to set sleep timing. Nature 555, 98-102 (2018). 1048 56. M. P. Fernandez et al., Sites of Circadian Clock Neuron Plasticity Mediate Sensory Integration and Entrainment. Curr Biol 30, 2225-2237 e2225 (2020). 1050 57. T. Yoshii, T. Todo, C. Wulbeck, R. Stanewsky, C. Helfrich-Forster, Cryptochrome is present in the compound eyes and a subset of Drosophila's clock neurons. J Comp Neurol 508, 952-966 (2008). 1053 58. T. Yoshii, C. Hermann, C. Helfrich-Forster, Cryptochrome-positive and -negative clock neurons in Drosophila entrain differentially to light and temperature. J Biol Rhythms 25, 387-398 (2010). 1056 59. E. Marder, D. Bucher, D. J. Schulz, A. L. Taylor, Invertebrate central pattern generation moves along. Curr Biol 15, R685-699 (2005). 1058 60. A. I. Selverston, J. P. Miller, Mechanisms underlying pattern generation in lobster stomatogastric ganglion as determined by selective inactivation of identified neurons. I. 		53.	
 1044 54. F. Guo <i>et al.</i>, Circadian neuron feedback controls the Drosophila sleepactivity profile. <i>Nature</i> 536, 292-297 (2016). 1046 55. S. Yadlapalli <i>et al.</i>, Circadian clock neurons constantly monitor environmental temperature to set sleep timing. <i>Nature</i> 555, 98-102 (2018). 1048 56. M. P. Fernandez <i>et al.</i>, Sites of Circadian Clock Neuron Plasticity Mediate Sensory Integration and Entrainment. <i>Curr Biol</i> 30, 2225-2237 e2225 (2020). 1050 57. T. Yoshii, T. Todo, C. Wulbeck, R. Stanewsky, C. Helfrich-Forster, Cryptochrome is present in the compound eyes and a subset of Drosophila's clock neurons. <i>J Comp</i> <i>Neurol</i> 508, 952-966 (2008). 1053 58. T. Yoshii, C. Hermann, C. Helfrich-Forster, Cryptochrome-positive and -negative clock neurons in Drosophila entrain differentially to light and temperature. <i>J Biol Rhythms</i> 25, 387-398 (2010). 1056 59. E. Marder, D. Bucher, D. J. Schulz, A. L. Taylor, Invertebrate central pattern generation moves along. <i>Curr Biol</i> 15, R685-699 (2005). 1058 60. A. I. Selverston, J. P. Miller, Mechanisms underlying pattern generation in lobster stomatogastric ganglion as determined by selective inactivation of identified neurons. I. 			
 Nature 536, 292-297 (2016). S. Yadlapalli <i>et al.</i>, Circadian clock neurons constantly monitor environmental temperature to set sleep timing. <i>Nature</i> 555, 98-102 (2018). M. P. Fernandez <i>et al.</i>, Sites of Circadian Clock Neuron Plasticity Mediate Sensory Integration and Entrainment. <i>Curr Biol</i> 30, 2225-2237 e2225 (2020). T. Yoshii, T. Todo, C. Wulbeck, R. Stanewsky, C. Helfrich-Forster, Cryptochrome is present in the compound eyes and a subset of Drosophila's clock neurons. <i>J Comp</i> <i>Neurol</i> 508, 952-966 (2008). S. T. Yoshii, C. Hermann, C. Helfrich-Forster, Cryptochrome-positive and -negative clock neurons in Drosophila entrain differentially to light and temperature. <i>J Biol Rhythms</i> 25, 387-398 (2010). E. Marder, D. Bucher, D. J. Schulz, A. L. Taylor, Invertebrate central pattern generation moves along. <i>Curr Biol</i> 15, R685-699 (2005). A. I. Selverston, J. P. Miller, Mechanisms underlying pattern generation in lobster stomatogastric ganglion as determined by selective inactivation of identified neurons. I. 			
 S. Yadlapalli <i>et al.</i>, Circadian clock neurons constantly monitor environmental temperature to set sleep timing. <i>Nature</i> 555, 98-102 (2018). M. P. Fernandez <i>et al.</i>, Sites of Circadian Clock Neuron Plasticity Mediate Sensory Integration and Entrainment. <i>Curr Biol</i> 30, 2225-2237 e2225 (2020). T. Yoshii, T. Todo, C. Wulbeck, R. Stanewsky, C. Helfrich-Forster, Cryptochrome is present in the compound eyes and a subset of Drosophila's clock neurons. <i>J Comp Neurol</i> 508, 952-966 (2008). T. Yoshii, C. Hermann, C. Helfrich-Forster, Cryptochrome-positive and -negative clock neurons in Drosophila entrain differentially to light and temperature. <i>J Biol Rhythms</i> 25, 387-398 (2010). E. Marder, D. Bucher, D. J. Schulz, A. L. Taylor, Invertebrate central pattern generation moves along. <i>Curr Biol</i> 15, R685-699 (2005). A. I. Selverston, J. P. Miller, Mechanisms underlying pattern generation in lobster stomatogastric ganglion as determined by selective inactivation of identified neurons. I. 		54.	
 temperature to set sleep timing. <i>Nature</i> 555, 98-102 (2018). M. P. Fernandez <i>et al.</i>, Sites of Circadian Clock Neuron Plasticity Mediate Sensory Integration and Entrainment. <i>Curr Biol</i> 30, 2225-2237 e2225 (2020). 57. T. Yoshii, T. Todo, C. Wulbeck, R. Stanewsky, C. Helfrich-Forster, Cryptochrome is present in the compound eyes and a subset of Drosophila's clock neurons. <i>J Comp</i> <i>Neurol</i> 508, 952-966 (2008). 1053 58. T. Yoshii, C. Hermann, C. Helfrich-Forster, Cryptochrome-positive and -negative clock neurons in Drosophila entrain differentially to light and temperature. <i>J Biol Rhythms</i> 25, 387-398 (2010). 1056 59. E. Marder, D. Bucher, D. J. Schulz, A. L. Taylor, Invertebrate central pattern generation moves along. <i>Curr Biol</i> 15, R685-699 (2005). 60. A. I. Selverston, J. P. Miller, Mechanisms underlying pattern generation in lobster stomatogastric ganglion as determined by selective inactivation of identified neurons. I. 			
 M. P. Fernandez <i>et al.</i>, Sites of Circadian Clock Neuron Plasticity Mediate Sensory Integration and Entrainment. <i>Curr Biol</i> 30, 2225-2237 e2225 (2020). T. Yoshii, T. Todo, C. Wulbeck, R. Stanewsky, C. Helfrich-Forster, Cryptochrome is present in the compound eyes and a subset of Drosophila's clock neurons. <i>J Comp</i> <i>Neurol</i> 508, 952-966 (2008). T. Yoshii, C. Hermann, C. Helfrich-Forster, Cryptochrome-positive and -negative clock neurons in Drosophila entrain differentially to light and temperature. <i>J Biol Rhythms</i> 25, 387-398 (2010). E. Marder, D. Bucher, D. J. Schulz, A. L. Taylor, Invertebrate central pattern generation moves along. <i>Curr Biol</i> 15, R685-699 (2005). A. I. Selverston, J. P. Miller, Mechanisms underlying pattern generation in lobster stomatogastric ganglion as determined by selective inactivation of identified neurons. I. 		55.	
 Integration and Entrainment. <i>Curr Biol</i> 30, 2225-2237 e2225 (2020). T. Yoshii, T. Todo, C. Wulbeck, R. Stanewsky, C. Helfrich-Forster, Cryptochrome is present in the compound eyes and a subset of Drosophila's clock neurons. <i>J Comp</i> <i>Neurol</i> 508, 952-966 (2008). T. Yoshii, C. Hermann, C. Helfrich-Forster, Cryptochrome-positive and -negative clock neurons in Drosophila entrain differentially to light and temperature. <i>J Biol Rhythms</i> 25, 387-398 (2010). E. Marder, D. Bucher, D. J. Schulz, A. L. Taylor, Invertebrate central pattern generation moves along. <i>Curr Biol</i> 15, R685-699 (2005). A. I. Selverston, J. P. Miller, Mechanisms underlying pattern generation in lobster stomatogastric ganglion as determined by selective inactivation of identified neurons. I. 			
 T. Yoshii, T. Todo, C. Wulbeck, R. Stanewsky, C. Helfrich-Forster, Cryptochrome is present in the compound eyes and a subset of Drosophila's clock neurons. <i>J Comp</i> <i>Neurol</i> 508, 952-966 (2008). T. Yoshii, C. Hermann, C. Helfrich-Forster, Cryptochrome-positive and -negative clock neurons in Drosophila entrain differentially to light and temperature. <i>J Biol Rhythms</i> 25, 387-398 (2010). E. Marder, D. Bucher, D. J. Schulz, A. L. Taylor, Invertebrate central pattern generation moves along. <i>Curr Biol</i> 15, R685-699 (2005). A. I. Selverston, J. P. Miller, Mechanisms underlying pattern generation in lobster stomatogastric ganglion as determined by selective inactivation of identified neurons. I. 		56.	•
 present in the compound eyes and a subset of Drosophila's clock neurons. <i>J Comp</i> <i>Neurol</i> 508, 952-966 (2008). T. Yoshii, C. Hermann, C. Helfrich-Forster, Cryptochrome-positive and -negative clock neurons in Drosophila entrain differentially to light and temperature. <i>J Biol Rhythms</i> 25, 387-398 (2010). E. Marder, D. Bucher, D. J. Schulz, A. L. Taylor, Invertebrate central pattern generation moves along. <i>Curr Biol</i> 15, R685-699 (2005). A. I. Selverston, J. P. Miller, Mechanisms underlying pattern generation in lobster stomatogastric ganglion as determined by selective inactivation of identified neurons. I. 			
 Neurol 508, 952-966 (2008). T. Yoshii, C. Hermann, C. Helfrich-Forster, Cryptochrome-positive and -negative clock neurons in Drosophila entrain differentially to light and temperature. <i>J Biol Rhythms</i> 25, 387-398 (2010). E. Marder, D. Bucher, D. J. Schulz, A. L. Taylor, Invertebrate central pattern generation moves along. <i>Curr Biol</i> 15, R685-699 (2005). A. I. Selverston, J. P. Miller, Mechanisms underlying pattern generation in lobster stomatogastric ganglion as determined by selective inactivation of identified neurons. I. 		57.	•
 1053 58. T. Yoshii, C. Hermann, C. Helfrich-Forster, Cryptochrome-positive and -negative clock neurons in Drosophila entrain differentially to light and temperature. <i>J Biol Rhythms</i> 25, 387-398 (2010). 1056 59. E. Marder, D. Bucher, D. J. Schulz, A. L. Taylor, Invertebrate central pattern generation moves along. <i>Curr Biol</i> 15, R685-699 (2005). 1058 60. A. I. Selverston, J. P. Miller, Mechanisms underlying pattern generation in lobster stomatogastric ganglion as determined by selective inactivation of identified neurons. I. 			
 neurons in Drosophila entrain differentially to light and temperature. <i>J Biol Rhythms</i> 25, 387-398 (2010). 59. E. Marder, D. Bucher, D. J. Schulz, A. L. Taylor, Invertebrate central pattern generation moves along. <i>Curr Biol</i> 15, R685-699 (2005). A. I. Selverston, J. P. Miller, Mechanisms underlying pattern generation in lobster stomatogastric ganglion as determined by selective inactivation of identified neurons. I. 			
 1055 387-398 (2010). 1056 59. E. Marder, D. Bucher, D. J. Schulz, A. L. Taylor, Invertebrate central pattern generation 1057 moves along. <i>Curr Biol</i> 15, R685-699 (2005). 1058 60. A. I. Selverston, J. P. Miller, Mechanisms underlying pattern generation in lobster 1059 stomatogastric ganglion as determined by selective inactivation of identified neurons. I. 		58.	
 1056 59. E. Marder, D. Bucher, D. J. Schulz, A. L. Taylor, Invertebrate central pattern generation 1057 moves along. <i>Curr Biol</i> 15, R685-699 (2005). 1058 60. A. I. Selverston, J. P. Miller, Mechanisms underlying pattern generation in lobster 1059 stomatogastric ganglion as determined by selective inactivation of identified neurons. I. 			
 1057 moves along. <i>Curr Biol</i> 15, R685-699 (2005). 1058 60. A. I. Selverston, J. P. Miller, Mechanisms underlying pattern generation in lobster 1059 stomatogastric ganglion as determined by selective inactivation of identified neurons. I. 			
105860.A. I. Selverston, J. P. Miller, Mechanisms underlying pattern generation in lobster1059stomatogastric ganglion as determined by selective inactivation of identified neurons. I.		59.	
1059 stomatogastric ganglion as determined by selective inactivation of identified neurons. I.		_	•
		60.	
1060 Pyloric system. Journal of neurophysiology 44, 1102-1121 (1980).			
	1060		Pyloric system. Journal of neurophysiology 44, 1102-1121 (1980).

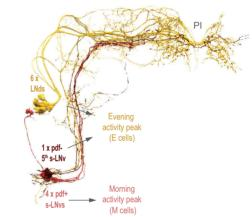
- 1061 61. A. L. Weaver, R. C. Roffman, B. J. Norris, R. L. Calabrese, A role for compromise:
 1062 synaptic inhibition and electrical coupling interact to control phasing in the leech
 1063 heartbeat CpG. *Front Behav Neurosci* 4 (2010).
- 1064 62. F. Nadim, S. Zhao, L. Zhou, A. Bose, Inhibitory feedback promotes stability in an oscillatory network. *J Neural Eng* **8**, 065001 (2011).
- 1066 63. L. K. Purvis, T. M. Wright, J. C. Smith, R. J. Butera, Significance of pacemaker vs. non1067 pacemaker neurons in an excitatory rhythmic network. *Conf Proc IEEE Eng Med Biol*1068 Soc 2006, 607-608 (2006).
- 1069 64. X. Liang, T. E. Holy, P. H. Taghert, Synchronous Drosophila circadian pacemakers 1070 display nonsynchronous Ca(2)(+) rhythms in vivo. *Science* **351**, 976-981 (2016).
- 1071 65. H. Dionne, K. L. Hibbard, A. Cavallaro, J. C. Kao, G. M. Rubin, Genetic Reagents for 1072 Making Split-GAL4 Lines in Drosophila. *Genetics* **209**, 31-35 (2018).
- 1073 66. B. K. Hulse *et al.*, A connectome of the Drosophila central complex reveals network
 1074 motifs suitable for flexible navigation and context-dependent action selection. *Elife* 10
 1075 (2021).
- 1076

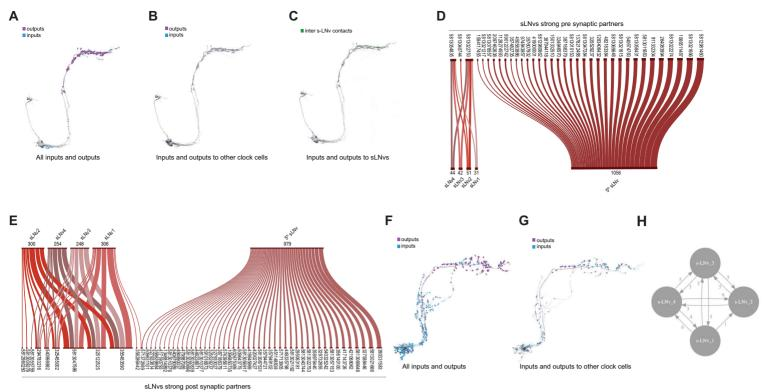


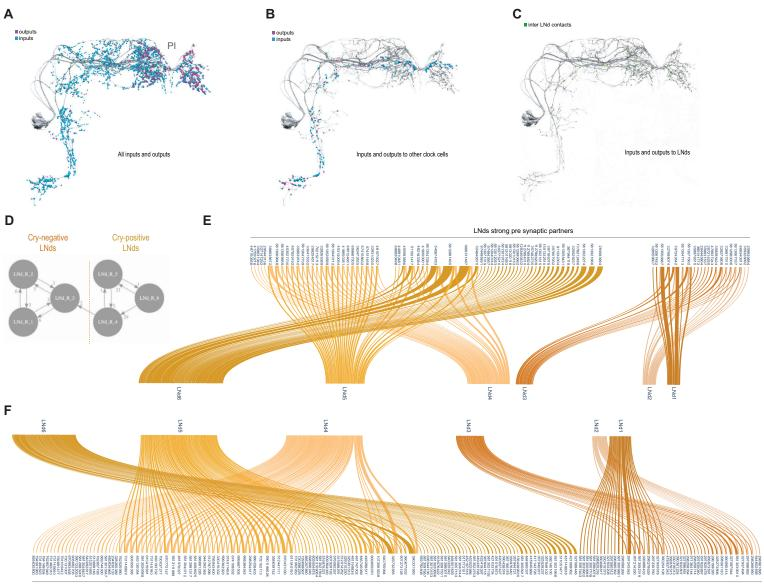




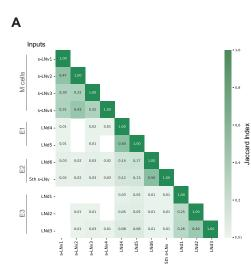
D

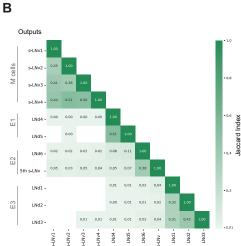


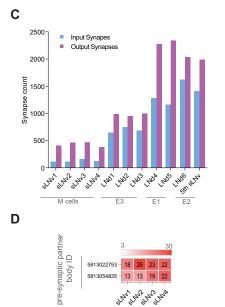




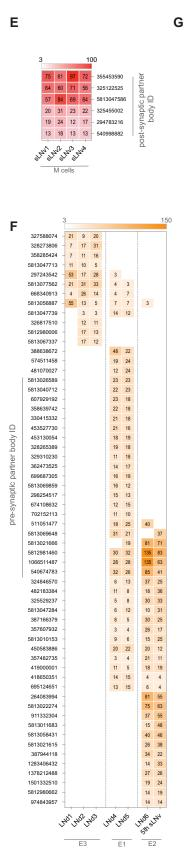
LNds strong post synaptic partners

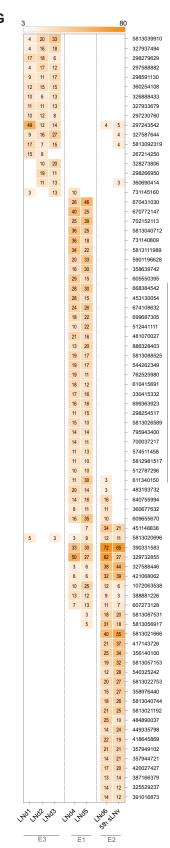






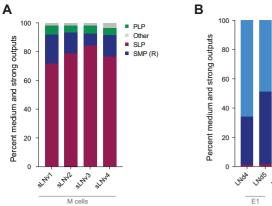
M cells

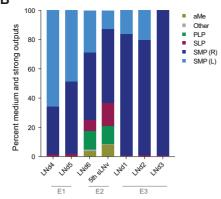




≙

post-synaptic partner body





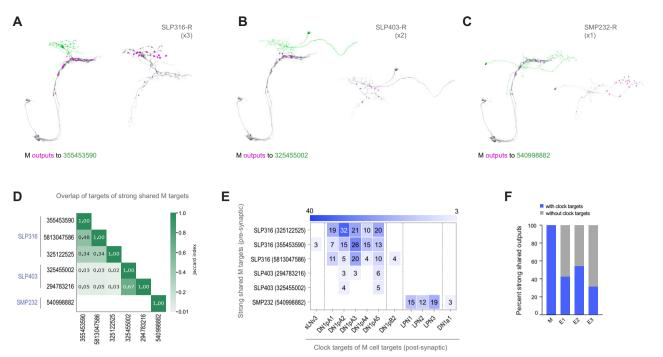
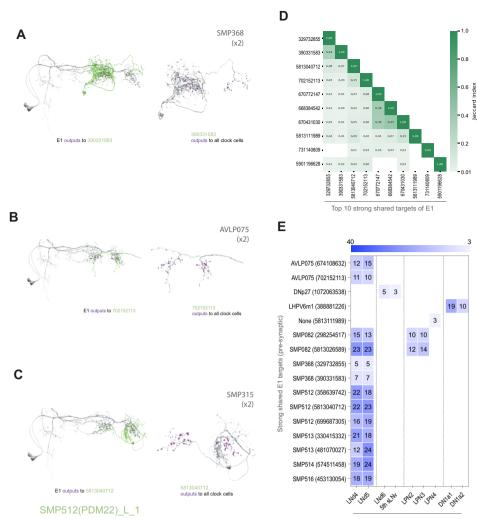
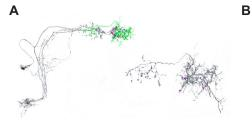


Figure 7



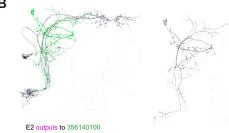
Clock targets of E1 strong shared targets (post-synaptic)



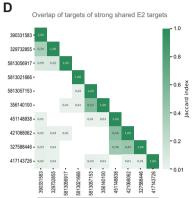
E2 outputs to 329732855

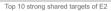
С

Ε



E2 outputs to 5813021666





DN1pA (325529237) 5 8 30 33 DN1pA (387166379) 5 30 25 8 LNd (5813021192) 5 Strong shared E2 outputs (pre-synaptic) SMP219 (420027427) 3 SMP222 (357949102) 3 5 SMP223 (417143726) 14 18 20 SMP223 (449335798) 7 3 4 5 SMP223 (540325242) 3 3 5 3 SMP223 (5813087531) 16 14 4 SMP368 (329732855) 55 SMP368 (390331583) 77 aMe (5813022753) - 18 26 23 22 23 16 25 16 8 6 29 16 20 21 aMe (5813040744) 9 12 8 9 11 3 81 71 aMe22 (5813021666)

Clock targets of E2 strong shared outputs (post-synaptic)

Figure 9.

